SIAM J. DISCRETE MATH.
Vol. 30, No. 2, pp. 801–831
© 2016 Society for Industrial and Applied Mathematics

SAMPLING AND COUNTING 3-ORIENTATIONS OF PLANAR TRIANGULATIONS*

SARAH MIRACLE†, DANA RANDALL‡, AMANDA PASCOE STREIB§, AND PRASAD TETALI¶

Abstract. Given a planar triangulation, a 3-orientation is an orientation of the internal edges so all internal vertices have out-degree three. Each 3-orientation gives rise to a unique edge coloring known as a *Schnyder wood* that has proven powerful for various computing and combinatorics applications. We consider natural Markov chains for sampling uniformly from the set of 3-orientations. First, we study a "triangle-reversing" chain on the space of 3-orientations of a fixed triangulation that reverses the orientation of the edges around a triangle in each move. We show that, when restricted to planar triangulations of maximum degree six, this Markov chain is rapidly mixing and we can approximately count 3-orientations. Next, we construct a triangulation with high degree on which this Markov chain mixes slowly. Finally, we consider an "edge-flipping" chain on the larger state space consisting of 3-orientations of all planar triangulations on a fixed number of vertices. We prove that this chain is always rapidly mixing.

Key words. Markov chains, 3-orientations, planar triangulations, Schnyder woods

AMS subject classification. 60J10

DOI. 10.1137/140965752

1. Introduction.

The 3-orientations of a graph have given rise to beautiful combinatorics and computational applications. A 3-orientation of a planar triangulation is an orientation of the internal edges of the triangulation such that every internal vertex has out-degree three. We study natural Markov chains for sampling 3-orientations in two contexts, when the triangulation is fixed and when we consider the union of all planar triangulations on a fixed number of vertices. When the triangulation is fixed, we allow moves that reverse the orientation of edges around a triangle if they form a directed cycle. We show that the chain is rapidly mixing (converging in polynomial time to equilibrium) if the maximum degree of the triangulation is six, but can be slowly mixing (requiring exponential time) if the degrees are unbounded. When the maximum degree of the triangulation is six, we give a FPRAS (fully polynomial randomized approximation scheme) for approximately counting the number of 3-orientations of the fixed triangulation. To sample from the set of all 3-orientations of triangulations with n vertices we use a simple "edge-flipping" chain and show it is always rapidly mixing. These chains arise in contexts such as sampling Eulerian orientations and triangulations of fixed planar point sets, so there is additional motivation for understanding their convergence rates.

*Received by the editors April 18, 2014; accepted for publication (in revised form) January 20, 2016; published electronically April 27, 2016. A preliminary version of this paper appeared in the *DMTCS Proceedings of the* 23*rd International Meeting on Probabilistic, Combinatorial, and Asymptotic Methods for the Analysis of Algorithms* [26].

http://www.siam.org/journals/sidma/30-2/96575.html

†Computer and Information Sciences, University of St. Thomas, Saint Paul, MN 55105 (sarah.miracle@stthomas.edu).

‡College of Computing, Georgia Institute of Technology, Atlanta, GA 30332-0765 (randall@cc.gatech.edu). This author's research was supported in part by NSF CCF-1219020.

§Center for Computing Sciences, Bowie, MD 20715-4300 (ampasco@super.org).

¶School of Mathematics and School of Computer Science, Georgia Institute of Technology, Atlanta, GA 30332-0765 (tetali@math.gatech.edu). This author's research was supported in part by NSF DMS-1101447 and CCR-0910584.

More precisely, given an undirected graph $G = (V, E)$ and a function $\alpha : V \to \mathbb{Z}^+$, an α-orientation is an orientation of E where each vertex v has out-degree $\alpha(v)$. Several fundamental combinatorial structures—spanning trees, bipartite perfect matchings, Eulerian orientations, etc.—can be seen as special instances of α-orientations of planar graphs. We refer the reader to [14, 15, 17] for extensive literature on the subject. Not surprisingly, counting α-orientations is $\#P$-complete. Namely, consider an undirected Eulerian graph G (with all even degrees); the α-orientations of G, where $\alpha(v) = d(v)/2$, correspond precisely to Eulerian orientations of G. The latter problem has been shown to be $\#P$-complete by Mihail and Winkler [25], and more recently Creed [10] showed that it remains $\#P$-complete even when restricted to planar graphs.

The term 3-*orientation* refers to an α-orientation of a planar triangulation where all *internal vertices* (vertices not bounding the infinite face) have $\alpha(v) = 3$ and all *external vertices* (the three vertices bounding the infinite face) have $\alpha(v) = 0$. Each 3-orientation gives rise to a unique edge coloring, known as a *Schnyder wood*, whose many combinatorial applications include graph drawing [28, 9] and poset dimension theory [29]. Several intriguing enumeration problems remain open, such as the complexity of enumerating 3-orientations of a planar triangulation (see, e.g., [17].) We study the problem of sampling 3-orientations of a fixed (planar) triangulation, as well as sampling 3-orientations of all triangulations with n internal vertices. In particular, we analyze the mixing times of two natural Markov chains for these problems, which were introduced previously but had thus far resisted analysis.

1.1. Results. First, we study the problem of sampling 3-orientations of a fixed triangulation with a particular natural Markov chain, which was stated as an open problem by Felsner and Zickfeld [17]. Although there is no known efficient method for counting exactly, there are polynomial-time algorithms for approximately counting and sampling 3-orientations due to a bijection with perfect matchings of a particular bipartite graph (see section 6.2 in [17]). This bijection allows us to sample 3-orientations in time $O^*(n^7)$ using an algorithm due to Bezáková et al. [2] (improving on the results of Jerrum, Sinclair, and Vigoda [20]), but this approach is indirect and intricate.

We consider instead a natural "triangle-reversing" Markov chain, $\mathcal{M}_\triangle$, that reverses the orientation of a directed triangle in each step, thus maintaining the out-degree at each vertex. Brehm [8] showed that for any fixed triangulation T, $\mathcal{M}_\triangle$ connects the state space $\Psi(T)$ of all 3-orientations of T. We also consider a related "cycle-reversing" chain, $\mathcal{M}_C$, that can also reverse directed cycles containing more than one triangle. The chain $\mathcal{M}_C$ is a nonlocal version of $\mathcal{M}_\triangle$ based on "tower moves" reminiscent of those in [23]. Let $\Delta_I(T)$ denote the maximum degree of any internal vertex of T. We prove that if T is a planar triangulation with $\Delta_I(T) \le 6$, then the Markov chain $\mathcal{M}_C$ on the state space $\Psi(T)$ is rapidly mixing. We then use a standard comparison argument together with the bound on the mixing time of $\mathcal{M}_C$ to infer a bound on the mixing time of the triangle-reversing chain $\mathcal{M}_\triangle$. We use the sampling algorithm $\mathcal{M}_C$ (or $\mathcal{M}_\triangle$) to approximately count 3-orientations of a fixed triangulation T using techniques based on [21]. Specifically, we prove that if T is a planar triangulation with $\Delta_I(T) \le 6$, then there exists a FPRAS for counting the number of 3-orientations of T.

Note that the class of planar triangulations with $\Delta_I \le 6$ is exponentially large in n, the number of vertices. An interesting related case is finite regions Λ of the triangular lattice, since sampling 3-orientations on Λ corresponds to sampling Eulerian orientations. Creed [10] solved the sampling problem in this case using a similar

approach based on towers; he shows that for certain subsets of the triangular lattice the tower chain can be shown to mix in time $O(n^4)$. In addition, it was previously shown that similar cycle-reversing chains are rapidly mixing in the context of sampling Eulerian orientations on the Cartesian lattice [23] and the 8-vertex model [13]. Our analysis here bounding the mixing time of $\mathcal{M}_C$ in the general setting of arbitrary planar graphs with maximum degree 6 requires additional combinatorial insights because we no longer have the regular lattice structure. In particular, we make use of a combinatorial structure outlined by Brehm [8]. In fact, this structure allows us to extend our analysis to certain non-4-connected triangulations that can have vertices of degree greater than six.

Next, we prove that when the maximum degree is unbounded, the chain $\mathcal{M}_\triangle$ may require exponential time. We prove that for any (large) n, there exists a triangulation T of size n for which the mixing time of $\mathcal{M}_\triangle$ and $\mathcal{M}_C$ on the state space $\Psi(T)$ is exponential in n. Based on the construction we give here, Felsner and Heldt [16] recently constructed another, somewhat simpler, family of graphs for which the mixing time of $\mathcal{M}_\triangle$ and $\mathcal{M}_C$ is exponentially large. However, we note that their family also has maximum degree that grows with n.

The second problem we study is sampling from the set of all 3-orientations arising from all possible triangulations on n internal vertices. Let Ψ_n be the set of all 3-orientations of triangulations of a labeled fixed point set with $n+3$ vertices, three of which are external vertices, where the edges of the triangulations are not required to be straight and the fixed positions of the points are arbitrary (i.e., all fixed positions result in the same set Ψ_n). The set Ψ_n is known to be in 1-1 correspondence with all pairs of noncrossing Dyck paths, and as such has size $C_{n+2}C_n - C_{n+1}^2$, where C_n is the nth Catalan number. Since exact enumeration is possible, we can sample using the reduction to counting; this was explicitly worked out by Bonichon and Mosbah [7]. We consider a natural Markov chain approach for sampling that in each step selects a quadrangle at random, removes the interior edge, and replaces it with the other diagonal in such a way as to restore the out-degree at each vertex. Bonichon, Le Saëc, and Mosbah [6] showed that the chain $\mathcal{M}_E$ connects the state space Ψ_n and we present the first bounds showing that the chain is rapidly mixing. Although the exact counting approach already yields a fast approach to sampling, the chain $\mathcal{M}_E$ is compelling because it arises in other contexts where we do not have methods to count exactly. For example, it has been proposed as a method for sampling triangulations of a fixed planar point set, a problem that has been open for over twenty years. Moreover, there is additional interest in the mixing time of this chain precisely because the number is related to the Catalan numbers; there has been extensive work trying to bound mixing times of natural Markov chains for various families of Catalan structures (see, e.g., [24]).

The primary challenge behind the proofs of these results is extracting the right combinatorial insights to understand the dynamics in the context of Schnyder woods and 3-orientations. Fortunately, there is a long history examining the rich structure of Schnyder woods. We extend these results in several new ways, allowing us to bound the mixing times of these chains. Our proof of rapid mixing for $\mathcal{M}_C$ involves a complex coupling argument that is straightforward if T is the triangular lattice, but requires more work to generalize to all triangulations with $\Delta_I \leq 6$. We then use $\mathcal{M}_C$ to construct an FPRAS by iteratively sampling and reducing to a triangulation with one fewer vertex. Our proof combines techniques introduced by [21] with special structural properties of 3-orientations. To prove our slow mixing result for $\mathcal{M}_\triangle$ and $\mathcal{M}_C$, we produce an intricate triangulation T which is carefully constructed to reveal

an exponentially small cut in the state space $\Psi(T)$. Although our choice of T may seem complicated, it was carefully designed using properties of 3-orientations to show that the Markov chain may be slow. Our proof of rapid mixing for $\mathcal{M}_E$ involves a detailed application of the comparison method to bound the mixing time of $\mathcal{M}_E$ by relating it to a local Markov chain on Dyck paths, $\mathcal{M}_D$, whose mixing time is known (see [23, 31]). The key obstacle here is decomposing moves of $\mathcal{M}_D$ into moves of $\mathcal{M}_E$ while avoiding congestion. This is especially challenging because although $\mathcal{M}_D$ is local in the setting of Dyck paths, in the context of 3-orientations it can make global changes to a 3-orientation in a single step.

2. Preliminaries. We begin with background on 3-orientations, Schnyder woods, and Markov chains. Fraysseix and Ossona de Mendez defined a bijection between $\Psi(T)$ and the Schnyder woods of T [18]. A *Schnyder wood* (see Figure 2.1b) is a 3-coloring and orientation of the internal edges of T such that for every internal vertex v,

- v has out-degree exactly 1 in each of the three colors: blue, red and green, and
- the clockwise order of the edges incident to v is outgoing green, incoming blue, outgoing red, incoming green, outgoing blue, and incoming red (see Figure 2.1a).

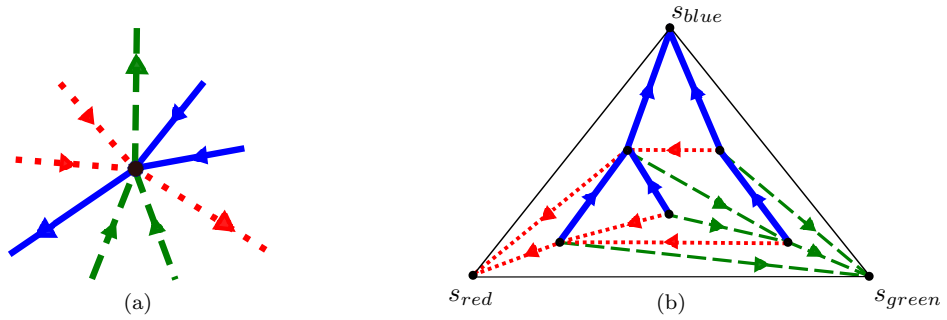

FIG. 2.1. (a) *The vertex condition.* (b) *An example Schnyder wood with nine internal vertices.*

In our figures, we differentiate the colors of edges in the Schnyder woods by dashed lines (green), dotted lines (red), and solid lines (blue). The external face is not oriented or colored. These conditions imply that each internal vertex has exactly one outgoing edge in each of the three colors and has zero or more incoming edges in each of the three colors. Notice the orientation of the edges of a Schnyder wood is a 3-orientation and each of the colors forms a directed tree which spans the internal vertices and is rooted at one of the external vertices. We refer to the roots of the red, blue, and green trees as s_{red}, s_{blue}, and s_{green}, respectively. Throughout the proofs, when we refer to the colors of the edges of a 3-orientation, we mean the colors of the Schnyder wood associated with that 3-orientation. We will use the additional information provided by the bijection with Schnyder woods extensively throughout the proofs. Note that given a 3-orientation there is a unique coloring that satisfies the Schnyder woods definition. Throughout the paper, we refer to an undirected edge of a triangulation as (x, y) and use the notation $\overrightarrow{xy}$ to refer to a directed edge that is part of some 3-orientation.

Next, we present some standard background on Markov chains. The time a Markov chain takes to converge to its stationary distribution π is measured in terms of the distance between π and $\mathcal{P}^t$, the distribution at time t. The *total variation*

distance at time t is

$$\|\mathcal{P}^t, \pi\|_{tv} = \max_{x \in \Psi} \frac{1}{2} \sum_{y \in \Psi} |\mathcal{P}^t(x, y) - \pi(y)|,$$

where $\mathcal{P}^t(x, y)$ is the t-step transition probability and Ψ is the state space. For all $\epsilon > 0$, the *mixing time* τ of $\mathcal{M}$ is defined as

$$\tau(\epsilon) = \min\{t : \|\mathcal{P}^{t'}, \pi\|_{tv} \leq \epsilon \, \forall t' \geq t\}.$$

We say that a Markov chain is *rapidly mixing* if the mixing time is bounded above by a polynomial in n and *slowly mixing* if it is bounded from below by an exponential in n. In this case, n is the number of internal vertices of the triangulations.

3. Sampling 3-orientations of a fixed triangulation. In this section, we consider a Markov chain for sampling the 3-orientations of a given triangulation. Let T be a planar triangulation with n internal vertices. Consider the following natural local Markov chain $\mathcal{M}_\triangle$ on the set of all 3-orientations of T. Select a directed triangle at random and reverse its orientation. We will see that $\mathcal{M}_\triangle$ samples from the uniform distribution, but its efficiency will depend on T. In section 3.2 we show that if the maximum degree of any internal vertex is at most 6, $\mathcal{M}_\triangle$ is rapidly mixing. Section 3.3 shows how to use $\mathcal{M}_\triangle$ to construct an FPRAS. In contrast, in section 3.4 we demonstrate a triangulation T with unbounded degree for which $\mathcal{M}_\triangle$ takes exponential time to sample from the state space $\Psi(T)$. Define $\mathcal{M}_\triangle$ as follows (see Figure 3.1).

The Markov chain $\mathcal{M}_\triangle$

Starting at any $\sigma_0 \in \Psi(T)$, iterate the following:

- Choose a triangle t in σ_i uniformly at random.
- If t is a directed cycle, with probability $1/2$ reverse t to obtain σ_{i+1}.
- Otherwise, $\sigma_{i+1} = \sigma_i$.

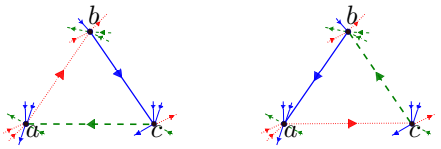

FIG. 3.1. *A move of $\mathcal{M}_\triangle$. The triangle $\triangle abc$ reverses to $\triangle acb$.*

Brehm proved $\mathcal{M}_\triangle$ connects the state space $\Psi(T)$ [8]. Since all valid moves have the same transition probabilities and all moves are reversible, $\mathcal{M}_\triangle$ converges to the uniform distribution over the state space $\Psi(T)$ (see, e.g., [30]).

3.1. Background on 3-orientations of planar triangulations. In this section we will provide an overview of several results on 3-orientations of planar triangulations and the Markov chain $\mathcal{M}_\triangle$ which we will use in section 3.2 to show that $\mathcal{M}_\triangle$ mixes rapidly when the maximum degree of the triangulation is at most 6. Brehm [8] provides a detailed analysis of the robust structure of 3-orientations of planar graphs. In particular, he constructs a framework which shows that the set of 3-orientations form a distributive lattice and that for a planar triangular graph G,

any two 3-orientations of G are connected by a series of moves of the Markov chain $\mathcal{M}_\triangle$. As part of this effort, Brehm examines a potential function on the faces of the graph, which we will see is useful to upper bound the number of 3-orientations for a given triangulation and the maximum distance between any two 3-orientations.

To show connectivity of $\mathcal{M}_\triangle$, Brehm first considers the case of 4-connected planar triangulations. In this case, every triangle of G is a face and he shows that it is possible to get between any two 3-orientations by a sequence of reversals of directed facial triangles. Suppose now that a planar triangulation G has exactly one nonfacial triangle t. For any nonfacial triangle, Brehm shows that in any 3-orientation of G, the edges in the region bounded by that triangle that are incident to some vertex v of the triangle must be directed towards v. This implies that no face f contained within t that shares an edge with t can be bounded by a directed triangle; hence such faces can never be reversed. In fact, this implies (see [8] for details) that G can be regarded as the cross product of the triangulation $G_{|t}$, the restriction of G to the three vertices on the boundary of t, and the vertices contained within the region bounded by t and the triangulation $G_{\backslash t}$ obtained by removing all vertices and edges contained within the region bounded by t. Thus by allowing $\mathcal{M}_\triangle$ to reverse arbitrary directed triangles (not just facial triangles), this amounts to extending $\mathcal{M}_\triangle$ to the triangulation $G_{\backslash t}$ which is now 4-connected. The same arguments will hold when G has many nonfacial triangles. Thus Brehm obtains the following theorem.

THEOREM 1 (Brehm). *For any planar triangulation G, the Markov chain $\mathcal{M}_\triangle$ connects the set of all 3-orientations of G.*

In our setting, we use the fact that $G_{|t}$ is independent of $G_{\backslash t}$ to show that the mixing time of $\mathcal{M}_\triangle$ is the maximum of the mixing times of each 4-connected piece of G, subject to the delay which results from the fact that $\mathcal{M}_\triangle$ only attempts to update one 4-connected piece at a time.

Brehm defines a *potential* X of a 4-connected planar triangulation as follows.

DEFINITION 1. *A* potential *X of a 4-connected planar triangulation G is a mapping $f \to x_f$ from the interior faces to the natural numbers such that*

- *$x_f = 0$ if the boundary of f contains an exterior edge,*
- *$|x_f - x_g| \le 1$ holds for any two adjacent faces f, g.*

The value *of a potential X is defined by $|X| = \sum_f x_f$.*

Let $d(\sigma, \tau)$ denote the minimum number of moves of $\mathcal{M}_\triangle$ to get between two 3-orientations σ and τ. For any 4-connected triangular graph G, there exists a minimal and a maximal 3-orientation σ_L and σ_R (so that $|\sigma_L| = 0$ and σ_R has the maximum value over all 3-orientations) [8]. It turns out that there is a bijection between 3-orientations of G and a subset of the potentials of G, called *induced* potentials, and that each move of $\mathcal{M}_\triangle$ changes the potential of a face by ± 1. The induced potential X of a 3-orientation σ_X of triangulation T is defined as follows: for each face f of T, x_f is the number of times the face f is flipped in a maximal flip sequence between σ_L and σ_X. Brehm shows that for any 3-orientation σ_X with induced potential X, the distance to the minimal triangulation satisfies $d(\sigma_X, \sigma_L) = |X| = \sum_f |x_f|$ and $d(\sigma_X, \sigma_R) = |\sigma_R| - |X|$ (see [8] for details). We need something stronger, which is that the distance between arbitrary 3-orientations is also given by the potential functions. We prove this in Proposition 1. First, we need the following lemma.

LEMMA 2. *Let σ_X and σ_Y be 3-orientations of triangulation T with induced potentials X and Y, respectively. Consider the function Δ on faces of T defined by $\delta_f = y_f - x_f$. Let f and g be two adjacent faces separated by edge e. If e has the*

same orientation in σ_X and σ_Y, then $\delta_f = \delta_g$, and otherwise $|\delta_f - \delta_g| = 1$.

Proof. We will use two key facts from [8]. First, if f is left of g in σ_X, then $x_f \geq x_g$. Second, by Theorem 2.4.2 of Brehm, $x_f = x_g$ if e has the same orientation in σ_X and σ_L. If e has the opposite orientation in σ_X from σ_L, then $|x_f - x_g| = 1$. Assume e has the same orientation in σ_X and σ_Y. Then either they both agree with σ_L on e, and so $x_f = x_g$ and $y_f = y_g$, which implies $\delta_f = \delta_g$, or they both disagree with σ_L on e, and so $x_f - x_g = \pm 1$ and $y_f - y_g = \pm 1$. In the latter case, $x_f > x_g$ implies f is left of g in σ_X, but since σ_X and σ_Y agree on e, this means f is left of g in σ_Y so $y_f > y_g$. Therefore, $\delta_f = \delta_g$. Now assume e has the opposite orientation in σ_X and σ_Y. Then $x_f - x_g = 0$ implies $y_f - y_g = \pm 1$, so $\delta_f - \delta_g = \pm 1$ and similarly if $y_f - y_g = 0$, then $x_f - x_g = \pm 1$, so $\delta_f - \delta_g = \pm 1$. ∎

PROPOSITION 1. *The distance in the face-flip Markov chain between σ_X and σ_Y is given by $\sum_f |x_f - y_f|$.*

Proof. Clearly the distance is at least $\sum_f |x_f - y_f|$, since each step of the Markov chain changes the sum by only one. To show that $\sum_f |x_f - y_f|$ steps is sufficient, we will show that there is always a face to flip that will decrease the sum by one.

Lemma 2 implies that the level sets of Δ are separated by cycles that have different orientations in σ_X and σ_Y. Let S be the maximum level set in Δ with bounding cycle C. Suppose without loss of generality that C is counterclockwise in σ_Y and clockwise in σ_X. Then by Corollary 1.5.2 of Brehm, there exists a clockwise triangle in S in σ_X, which upon rotation creates $\sigma_{X'}$ that is one step closer to σ_Y. ∎

This implies that the distance between σ_X and σ_Y is at most $d(\sigma_L, \sigma_R) = |R|$. To bound this distance, it suffices to bound $|R|$. Every triangulation $G \in \mathcal{T}_n$ has $2n + 1$ faces (not counting the infinite face). It is easy to see that for any potential of G, the maximum value for any face is at most $\lfloor \frac{2n+1}{2} \rfloor$ since each face can only differ from its neighbors by at most 1 and faces adjacent to the boundary have value 0. This implies Corollary 3(a). Moreover, the number of 3-orientations of a graph G is bounded by the number of induced potentials of G. Since each face in a potential is within 1 from each of its adjacent faces, the number of induced potentials is at most 3^{2n+1}.

COROLLARY 3. *Let G be a 4-connected planar triangulation.*
(a) *The maximum distance between two 3-orientations of G is at most $(2n+1)^2/2$.*
(b) *The number of 3-orientations of G is at most 3^{2n+1}.*

3.2. Fast mixing of $\mathcal{M}_\triangle$ for maximum degree at most 6. In this section we prove that $\mathcal{M}_\triangle$ is rapidly mixing on the state space $\Psi(T)$ if T is a planar triangulation with $\Delta_I(T) \leq 6$. First, we introduce an auxiliary chain $\mathcal{M}_C$, which we will then use to derive a bound on the mixing time of $\mathcal{M}_\triangle$. The Markov chain $\mathcal{M}_C$ involves *towers* of moves of $\mathcal{M}_\triangle$, based on the nonlocal chain introduced in [23]. Notice that if a face f cannot move (i.e., f is not bounded by a directed cycle), then two of its edges have the same orientation and the other edge does not. We call this edge the *disagreeing edge* of f. We define a *tower of length k* as follows.

DEFINITION 2. *A tower of length k is a path of faces $f_1, f_2, \ldots, f_k$ such that the following three conditions are met:*
- *f_k is the only face which is bounded by a directed cycle (i.e., it has a move);*
- *for every $1 \leq i < k$, the disagreeing edge of f_i is incident to f_{i+1};*
- *and every vertex v is incident to at most three consecutive faces in the path (see Figure 3.2).*

The idea of the tower is that once the edges of f_k are reversed, then the edges of f_{k-1} can be reversed, and so on. We call f_1 the *beginning* of the tower, and f_k the *end*. Notice that every face is the beginning of at most one tower (it may be a tower of length 1). The effect of making these moves is to reverse the edges of the directed cycle surrounding the path of faces $f_1, f_2, \ldots, f_k$ (although the colors on the internal edges also change); we will refer to this move as *reversing the tower*. The *direction* of a tower is the direction of the directed cycle surrounding the path of faces. The Markov chain $\mathcal{M}_C$ operates as follows.

The tower Markov chain $\mathcal{M}_C$

Starting at any σ_0, iterate the following:

- Choose a (finite) face f in σ_i and a direction d uniformly at random.
- If f is the beginning of a tower of length k with direction d, then with probability $\begin{cases} \frac{1}{3k}: & k \geq 2 \\ 1: & k = 1 \end{cases}$ reverse the tower to obtain σ_{i+1}.
- Otherwise, $\sigma_{i+1} = \sigma_i$.

The moves of $\mathcal{M}_\triangle$ are a subset of the moves of $\mathcal{M}_C$, so $\mathcal{M}_C$ is also connected.

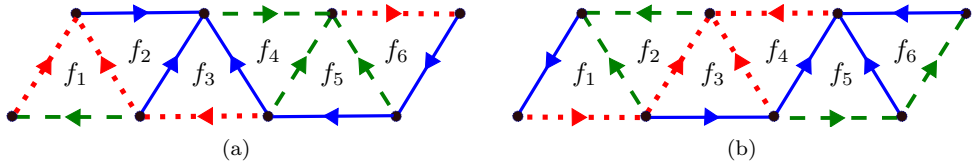

FIG. 3.2. *A move of the tower chain with beginning f_1, end f_6, and length 6 from* (a) *to* (b).

We first consider the case that T is 4-connected, then we apply the comparison theorem to prove that $\mathcal{M}_C$ is also rapidly mixing and extend the result to non-4-connected triangulations using a result of Brehm [8]. Notice if T is 4-connected, every triangle is facial, so $\mathcal{M}_\triangle$ selects a face and reverses the directions of the edges around that face if possible. The bulk of the work to prove rapid mixing of $\mathcal{M}_C$ and $\mathcal{M}_\triangle$ is to show that $\mathcal{M}_C$ is rapidly mixing when T is 4-connected. The main tool we use in the case where T is 4-connected is the following path coupling theorem due to Dyer and Greenhill [12].

THEOREM 4 (Dyer and Greenhill). *Let d be an integer-valued metric on $\Psi \times \Psi$ which takes values in $\{0, \ldots, B\}$. Let U be a subset of $\Psi \times \Psi$ such that for all $(\sigma, \tau) \in \Psi \times \Psi$ there exists a path $\sigma = z_0, z_1, \ldots, z_r = \tau$ between σ and τ such that $(z_i, z_{i+1}) \in U$ for $0 \leq i < r$ and $\sum_{i=0}^{r-1} d(z_i, z_{i+1}) = d(\sigma, \tau)$. Let $\mathcal{M}$ be a Markov chain on state space Ψ with transition matrix P. Consider any random function $f : \Psi \to \Psi$ such that $\Pr[f(\sigma) = \tau] = P(\sigma, \tau)$ for all $\sigma, \tau \in \Psi$, and define a coupling of the Markov chain by $(\sigma_t, \tau_t) \to (\sigma_{t+1}, \tau_{t+1}) = (f(\sigma_t), f(\tau_t))$. Let $\alpha > 0$ satisfy $\mathbb{E}[(d(\sigma_{t+1}, \tau_{t+1}) - d(\sigma_t, \tau_t))^2] \geq \alpha$ for all t such that $\sigma_t \neq \tau_t$.[1] Suppose $E[d(\sigma_{t+1}, \tau_{t+1})] \leq d(\sigma_t, \tau_t)$, for*

[1]Note the original theorem of Dyer and Greenhill makes the stronger assumption $\Pr[d(\sigma_{t+1}, \tau_{t+1}) \neq d(\sigma_t, \tau_t)] \geq \alpha$ for all t such that $\sigma_t \neq \tau_t$, and then uses this to show that $\mathbb{E}[(d(\sigma_{t+1}, \tau_{t+1}) - d(\sigma_{t+1}, \tau_{t+1}))^2] \geq \alpha$. We require the weaker assumption here, but the proof is identical.

all $\sigma_t, \tau_t \in U$. Then the mixing time of the chain $\mathcal{M}$ on the state space Ψ satisfies

$$\tau(\epsilon) \leq 2 \left\lceil \frac{eB^2}{\alpha} \right\rceil \lceil \ln \epsilon^{-1} \rceil.$$

Notice Theorem 4 requires a bound on the variance of the distance. We prove the following bound, as long as the triangulation T has maximum degree at most 6.

LEMMA 5. *Let T be a triangulation with maximum degree at most 6, and let $\sigma_X^{(t-1)}$ and $\sigma_Y^{(t-1)}$ be two 3-orientations of T at time $t-1$. Then, for the tower Markov chain $\mathcal{M}_C$ with the trivial coupling,*

$$\mathbb{E}\left[\left|d\left(\sigma_X^{(t)}, \sigma_Y^{(t)}\right) - d\left(\sigma_X^{(t-1)}, \sigma_Y^{(t-1)}\right)\right|^2\right] \geq \frac{1}{6(2n+1)}.$$

Proof. Let $X = X_{t-1}$ and $Y = Y_{t-1}$ be the potential functions corresponding to 3-orientations $\sigma_X = \sigma_X^{(t-1)}$ and $\sigma_Y = \sigma_Y^{(t-1)}$. We will show that there is always a tower move of length k that changes the distance by k and succeeds in exactly one of σ_X and σ_Y. Assume this is true. If $k \geq 2$, then the Markov chain $\mathcal{M}_C$ chooses this tower move with probability at least $1/(4n+2)$ and it succeeds with probability $1/(6k)$ (and fails in the other 3-orientation, changing the distance by k). In this case the expected value of $(d(\sigma_X^{(t)}, \sigma_Y^{(t)}) - d(\sigma_X^{(t-1)}, \sigma_Y^{(t-1)}))^2$ is at least $k/(12(2n+1)) \geq 1/(6(2n+1))$. If $k = 1$, then the Markov chain $\mathcal{M}_C$ chooses this tower move with probability at least $1/(4n+2)$ and it succeeds with probability $1/2$ (and fails in the other 3-orientation). In this case the expected value of $(d(\sigma_X^{(t)}, \sigma_Y^{(t)}) - d(\sigma_X^{(t-1)}, \sigma_Y^{(t-1)}))^2$ is at least $1/(4(2n+1))$. This proves $\mathbb{E}[|d(\sigma_X^{(t)}, \sigma_Y^{(t)}) - d(\sigma_X^{(t-1)}, \sigma_Y^{(t-1)})|^2] \geq \frac{1}{6(2n+1)}$, as desired.

It remains to show that there is always a tower move of length k that changes the distance by k and succeeds in exactly one of σ_X and σ_Y. As before, let S be the maximum level set in Δ with bounding cycle C. Suppose without loss of generality that C is counterclockwise in σ_Y and clockwise in σ_X. Note that all edges internal to S have the same orientation in σ_X and σ_Y. Moreover, for any face f in S with an edge e that has the opposite orientation in σ_X from σ_Y, the edge e is on C and therefore is counterclockwise with respect to f in σ_Y and clockwise with respect to f in σ_X.

Let f_0 be a face in S incident to C. We will prove that there is a counterclockwise tower move in σ_Y or a clockwise tower move in σ_X beginning at f_0 that consists entirely of faces of S. This implies that upon rotating the tower, the distance decreases by k, if k is the length of the tower.

If f_0 is incident to at least two edges of C, then f_0 is a directed cycle in either σ_X or σ_Y, or both; however, if it is a directed cycle in both, then it has the opposite orientation in σ_X and σ_Y. Therefore, this tower (of length one) succeeds in one but not the other.

Suppose instead that f_0 is incident to exactly one edge, say e_0, of C. The other two edges of f_0 are the same orientation in σ_X and σ_Y. If they are both counterclockwise with respect to f_0 or both clockwise with respect to f_0, then f_0 is a directed cycle in either σ_X or σ_Y (but not both), and so as before we are done. Therefore, we may assume that the other two edges of f_0 (which share a vertex v_0) are either both directed out from v_0 or both directed into v_0 in both σ_X and σ_Y. Figure 3.3 illustrates each of these cases. Let e_1 be the disagreeing edge of f_0 for σ_Y, and let e_1' be the disagreeing edge of f_0 for σ_X. Let f_1 (f_1') be the other face incident to e_1 (resp., e_1'). Note that f_1 and f_1' are in S, since e_1 and e_1' are not on C. Moreover, e_1 is

counterclockwise with respect to f_1 and e_1' is clockwise with respect to f_1' in both σ_X and σ_Y. Consider the other edges incident to v_0. Let e_2 (e_2') be the other edge of f_1 (resp., f_1') incident to v_0. We claim that either e_2 is counterclockwise with respect to f_1 in σ_Y or e_2' is clockwise with respect to f_1' in σ_X. We consider two cases. Case 1: either e_2 or e_2' is on C. Suppose, for instance, that e_2 is on C. Since $f_1 \in S$, e_2 must be directed counterclockwise with respect to f_1 in σ_Y. Case 2: Now assume e_2 and e_2' are both internal edges in S, so that σ_X and σ_Y agree on both e_2 and e_2'. Since the maximum degree of T is at most 6, there are at most 3 out-edges of v_0 and at most 3 in-edges to v_0. If e_1 and e_1' are both out-edges of v_0, then at least one of e_2 and e_2' is an in-edge to v_0 in both σ_X and σ_Y. If it is e_2, then e_2 is counterclockwise with respect to f_1 and if it is e_2', then e_2' is clockwise with respect to f_1'. A similar argument shows the claim when e_1 and e_1' are both in-edges of v_0.

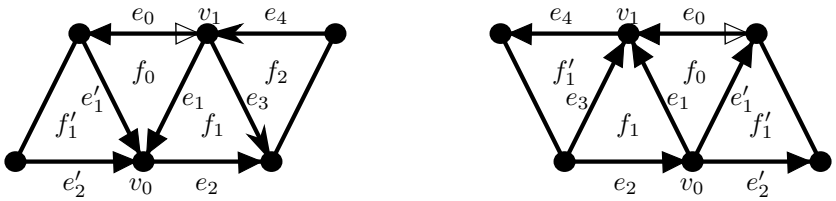

FIG. 3.3. *The beginning of the tower. The edges of σ_Y have bold arrows; the edge e_0 has a different orientation in σ_X, as indicated with an empty arrow. All other edges with orientations are the same in σ_X and σ_Y.*

Assume without loss of generality that e_2 is counterclockwise with respect to f_1 in σ_Y. We will define a tower move in σ_Y beginning in f_0. In the remainder of the proof, we consider only edges of σ_Y. We have already defined f_0, f_1, v_0, e_0, e_1, and e_2. Suppose we have defined the ith face of the tower: f_i, for $i > 0$. If f_i is a directed cycle, then it is the end of the tower; otherwise, let e_{2i+1} be the disagreeing edge of f_i and define f_{i+1} to be the other face incident to e_{2i+1}. Let v_i be the vertex that e_{2i-1} and e_{2i+1} share, and let e_{2i+2} be the other edge in f_{i+1} incident to v_i (see Figure 3.4).

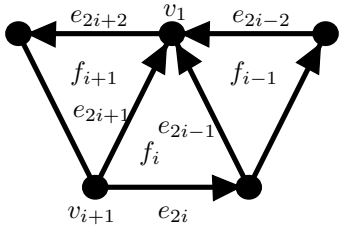

FIG. 3.4. *The middle of the tower. All edges are in σ_Y.*

We will prove by induction that for all faces f_i in the tower, $f_i \in S$ and e_{2i-1} and e_{2i} are counterclockwise with respect to f_i. We have already proved the base case, with $i = 1$. Now suppose the claim holds for some $i \geq 1$. If e_{2i+1} is on C, then f_i is a counterclockwise cycle in σ_Y and f_i is the end of the tower. Otherwise, f_{i+1} is in S and e_{2i+1} is clockwise with respect to f_i (since it is the disagreeing edge of f_i). This implies e_{2i+1} is counterclockwise with respect to f_{i+1}. Notice v_i has 3 in-edges or 3 out-edges (namely, e_{2i-2}, e_{2i-1}, and e_{2i+1}), so the other edge e_{2i+2} in f_{i+1} incident to v_i is the opposite direction. This shows that e_{2i+2} is counterclockwise with respect to f_{i+1}.

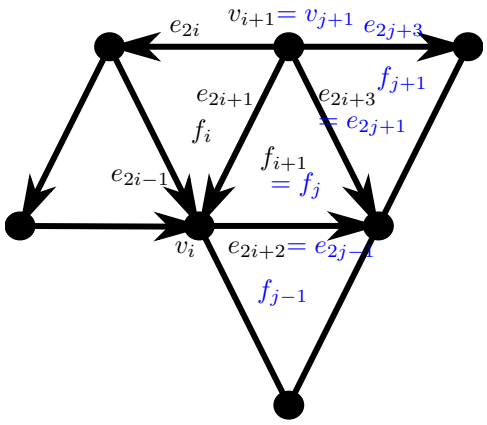

FIG. 3.5. *The middle of the tower. All edges are in* σ_Y.

In order for the tower to be a valid move of $\mathcal{M}_C$, the faces must form a path; that is, $f_i \neq f_j$ for all $j < i$. This is clearly true for $i = 1$. Suppose the claim holds for some $i \geq 1$. If f_{i+1} is a directed cycle, then clearly f_{i+1} is the first such face along the tower. If f_{i+1} contains an edge of C, then f_{i+1} is a directed cycle; this shows $f_{i+1} \neq f_0$. Suppose $f_{i+1} = f_j$ for some $1 \leq j < i+1$, as depicted in Figure 3.5. Hence the final edge e_{2i+3} of f_{i+1} is the disagreeing edge of $f_{i+1} = f_j$. This implies that f_{j+1} is incident to $e_{2i+3} = e_{2j+1}$. We have shown that for any $i > 0$, e_{2i-1} and e_{2i} are counterclockwise with respect to f_i. Hence e_{2j+3} is counterclockwise with respect to f_{j+2} and thus clockwise with respect to f_{j+1}. Therefore, vertex $v_{j+1} = v_{i+1}$ has 4 out-edges or 4 in-edges, namely $e_{2i}, e_{2i+1}, e_{2i+3} = e_{2j+1}$, and e_{2j+3}. This is a contradiction, since the maximum degree is at most 6 and every vertex has out-degree 3. ∎

We are now ready to use Theorem 4 to prove the following theorem.

THEOREM 6. *Let T be a 4-connected planar triangulation with $\Delta_I(T) \leq 6$. Then the mixing time of $\mathcal{M}_C$ on the state space $\Psi(T)$ satisfies $\tau(\epsilon) = O(n^5 \ln \epsilon^{-1})$.*

Proof. Let T be a 4-connected planar triangulation with $\Delta_I(T) \leq 6$. First, we prove that $\mathcal{M}_C$ is rapidly mixing on $\Psi(T)$. Define the distance d between any two 3-orientations in $\Psi(T)$ to be the minimum number of steps of $\mathcal{M}_\triangle$ from one to the other. Assume $\sigma = \sigma_t, \tau = \tau_t \in \Psi(T)$, and τ is obtained from σ by reversing a facial triangle f. We use the trivial coupling, which chooses the same face for σ and τ at every step. Suppose without loss of generality that the edges of f are clockwise in σ. In order to apply Theorem 4, we first show that the expected change in distance is at most 0, implying that $\mathbb{E}[d(\sigma_{t+1}, \tau_{t+1})] \leq d(\sigma_t, \tau_t)$. There are two obvious moves that decrease the distance, namely when the $\mathcal{M}_C$ selects the face f and chooses to direct the cycle clockwise or counterclockwise, each of which happens with probability $1/(2(2n+1))$. Moreover, any move of $\mathcal{M}_C$ that does not involve an edge of f occurs with the same probability in σ and τ, and hence is neutral (i.e., does not change the distance).

We call a tower *bad* if it does not end in f and it contains a neighbor f' of f that is not the end of the tower. In this case, we say this bad tower is *associated with* f'. On the other hand, a tower is *good* if it ends in f, or if it ends in a face f' adjacent to f and contains no other faces adjacent to f. We will show that the good towers in

σ have corresponding good towers in τ, while the bad towers in σ fail in τ (similarly, bad towers in τ fail in σ). Both good and bad towers can increase the distance. Any tower that is neither good nor bad does not contain an edge of f, so it is neutral with respect to the distance.

Suppose $k \geq 1$, $(f_1, f_2, \ldots, f_k)$ is a good tower in σ, and f_k is adjacent to f. Given these conditions, we claim that $(f_1, f_2, \ldots, f_k, f)$ is a good tower in τ. It is clear that in τ, f is the only one of these faces that is bounded by a cycle, and that upon rotating f, the tower $(f_1, f_2, \ldots, f_k)$ is possible. We must check two things: that $(f_1, f_2, \ldots, f_k, f)$ is a path of faces (i.e., does not contain any cycle of faces), and that every vertex is incident to at most three consecutive faces. The first condition is clear, since f_k is the only neighbor of f in $\{f_1, f_2, \ldots, f_k\}$, and $(f_1, f_2, \ldots, f_k)$ is a path of faces. Suppose the second condition does not hold. Then there is a vertex v incident to f, f_k, f_{k-1}, and f_{k-2}. The edges between faces f_{k-2} and f_{k-1} and between f_{k-1} and f_k are either both incoming to v or both outgoing from v (see Figure 3.6). Moreover, since the edge between f_{k-2} and f_{k-1} is the disagreeing edge of f_{k-2}, the two edges of f_{k-2} incident to v are either both incoming to v or both outgoing from v (similarly the two edges of f_k incident to v are either both incoming to v or both outgoing). Hence, there are four edges incident to v which are all incoming or all outgoing, a contradiction since a vertex of degree at most 6 with exactly three outgoing edges can have at most three incoming edges as well. Therefore, if a good tower of length $k \geq 1$ begins on a face f_1 and ends on a neighbor f_k of f in σ, then there is a corresponding tower of length $k+1$ that begins on f_1 and ends on f in τ.

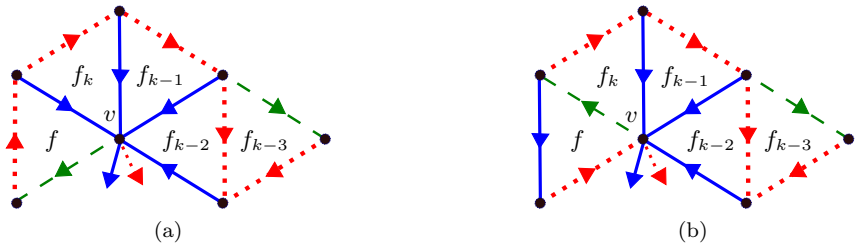

FIG. 3.6. *A tower* $(f_1, f_2, \ldots, f_k)$ *in* σ *for which* $(f_1, f_2, \ldots, f_k, f)$ *is not a tower in* τ. *Notice* $\deg(v) \geq 7$.

Thus we have shown that if $(f_1, f_2, \ldots, f_k)$ is a good tower in σ, then $(f_1, f_2, \ldots, f_k, f)$ is a good tower in τ. On the other hand, it should be clear that if $(f_1, f_2, \ldots, f_k, f)$ is a good tower of length $k+1 \geq 2$ that ends on f in σ, then $(f_1, f_2, \ldots, f_k)$ is a good tower of length k in τ. In either case, if $k \geq 2$, then the expected change in distance given the choice of these towers is

$$\left(-\frac{1}{3(k+1)} + k\left(\frac{1}{3k} - \frac{1}{3(k+1)}\right)\right) = 0.$$

If $k = 1$, then the expected change in distance given the choice of these towers is

$$-\frac{1}{6} + \left(1 - \frac{1}{6}\right) = \frac{2}{3}.$$

We point out that if σ and τ have good towers using a neighbor f' of f, then no bad tower in σ or τ is associated with f'; that is, if there exists a bad tower containing

f', then f' is the end of the tower. Suppose without loss of generality that the good tower is longer in τ than in σ. Then the edge between f and f' is the disagreeing edge of f' in τ so the only way to tower is towards f, so f' is not in a bad tower in τ. On the other hand, in σ, f' is bounded by a cycle, so it must be the end of any tower containing it.

Moreover, σ and τ can have at most two bad towers associated with a given face f' adjacent to f. It is clear that σ (resp., τ) has at most one bad tower that begins in f', which is defined by the disagreeing edge of f' in σ. However, σ may have a bad tower that uses f' but does not begin in f'. Let $(f_1, f_2, \ldots, f_k)$ be such a tower. We will show that $f' = f_2$; suppose not, so that $f' = f_i$, where $i \geq 3$. Then as above, there is a vertex v that is incident to f, f_i, f_{i-1}, and f_{i-2}, and the same proof will show that v must have either in-degree at least 4 or out-degree at least 4, which is a contradiction. Therefore, bad towers associated with f' must either begin in f' or in at most one neighbor $f_1 \neq f$ of f'. If there is a bad tower in σ (τ) beginning at f' and another beginning at some neighbor $f_1 \neq f$ (of f'), then in both σ and τ, the edge between faces f' and f_1 is f_1's disagreeing edge, which means that τ (resp., σ) cannot have a bad tower beginning in f' or using f' (since any such tower would have to go in a different direction than σ (resp., τ), toward f_1 since f' is adjacent to f). So if there are two bad towers in σ (τ) associated with f', then there are none in $\tau(\sigma)$. Therefore, there are at most two bad towers in σ or τ associated with f'. The contribution to the expected change in distance due to each bad tower of length $k \geq 2$ is

$$\frac{1}{2(2n+1)}\left(\frac{k}{3k}\right) = \frac{1}{2(2n+1)}\left(\frac{1}{3}\right).$$

We have shown that for any adjacent face f', there is either a good tower and no bad towers associated with f' (in which case the expected change in distance given that choice of tower is 2/3), or at most two associated bad towers (each of which has an expected change in distance of 1/3). Combining these observations, and summing over the three faces adjacent to f, the overall expected change in distance can be bounded as follows:

$$\mathbb{E}[\Delta d] \leq \frac{1}{2(2n+1)}\left[-2 + 3\left(\frac{2}{3}\right)\right] = 0.$$

Finally, by Lemma 5, we have

$$\mathbb{E}[(d(\sigma_t, \tau_t) - d(\sigma_{t+1}, \tau_{t+1}))^2] \geq 1/6(4n+2) =: \alpha.$$

By the path coupling theorem (Theorem 4) and the bound on B, the distance between any two 3-orientations, given in Corollary 3(a), we see the mixing time of $\mathcal{M}_C$ over 4-connected triangulations satisfies

$$\tau(\epsilon) \leq 2\left\lceil \frac{eB^2}{\alpha} \right\rceil \lceil \ln \epsilon^{-1} \rceil = 2\left\lceil \frac{e((2n+1)^2/2)^2}{1/6(4n+2)} \right\rceil \lceil \ln \epsilon^{-1} \rceil = O(n^5 \ln \epsilon^{-1}). \qquad \square$$

Next, we bound the mixing time of $\mathcal{M}_\triangle$ and $\mathcal{M}_C$ in the case of general planar triangulations. We will use Theorem 6 and the comparison method to bound the mixing time of $\mathcal{M}_\triangle$ in terms of the mixing time of $\mathcal{M}_C$ in the case of 4-connected triangulations.

The comparison theorem of Diaconis and Saloff-Coste [11] relates the mixing times of two reversible Markov chains P and P' on the state space Ψ. Suppose P and P'

have the same stationary distribution π and mixing times τ and τ', respectively. Let $E(P) = \{(X,Y) : P(X,Y) > 0\}$ and $E(P') = \{(X,Y) : P'(X,Y) > 0\}$ denote the transitions of the two Markov chains, viewed as directed graphs. For each $X, Y \in \Psi$ with $P'(X,Y) > 0$, define a canonical path $\gamma_{XY} = (X = X_0, X_1, \ldots, X_k = Y)$ with $P(X_i, X_{i+1}) > 0$ for $0 \le i < k$, and let $k = |\gamma_{XY}|$ denote the length. Let $\Gamma(Z,W) = \{(X,Y) \in E(P') : (Z,W) \in \gamma_{XY}\}$ be the set of canonical paths that use the transition (Z,W) of P. Let $\pi_* = \min_{X\in\Psi} \pi(X)$. Finally, define

$$A = \max_{(Z,W)\in E(P)} \sum_{(X,Y)\in\Gamma(Z,W)} |\gamma_{XY}|\pi(X)P'(X,Y)/(\pi(Z)P(Z,W)).$$

We will use the following version of the comparison theorem, due to Randall and Tetali [27].

THEOREM 7 (Randall and Tetali). *With the above notation, $0 < \epsilon < 1/2$, the mixing time of the Markov chain P on the state space Ψ satisfies*

$$\tau(\epsilon) \le 4\frac{\log(\frac{1}{\epsilon\pi_*})}{\log(1/(2\epsilon))} A\tau'(\epsilon).$$

We will extend the analysis to all planar triangulations by showing that $\mathcal{M}_\triangle$ operates as a product of independent Markov chains, each acting on a 4-connected planar triangulation. Thus, we will need one final detail, which is the following straightforward theorem, proved in [3] (similar results can also be found in [1, 4] and Corollary 12.12 of [22]).

THEOREM 8. *Suppose the Markov chain $\mathcal{M}$ is a product of M independent Markov chains $\mathcal{M}_1, \mathcal{M}_2, \ldots, \mathcal{M}_M$, where $\mathcal{M}$ updates $\mathcal{M}_i$ with probability p_i, where $\sum_i p_i = 1$. If $\tau_i(\epsilon)$ is the mixing time for $\mathcal{M}_i$ on the state space Ψ, then the mixing time of $\mathcal{M}$ on the state space Ψ satisfies*

$$\tau(\epsilon) \le \max_{i=1,2,\ldots,M} \max\left\{ \frac{2}{p_i}\ \tau_i\left(\frac{\epsilon}{2M}\right), \frac{8}{p_i}\ \ln\left(\frac{\epsilon}{8M}\right)\right\}.$$

We are now ready to bound the mixing time of $\mathcal{M}_C$ and $\mathcal{M}_\triangle$ for general planar triangulations.

THEOREM 9. *If T is a planar triangulation with $\Delta_I(T) \le 6$, then the mixing time of $\mathcal{M}_\triangle$ on the state space $\Psi(T)$ satisfies*

$$\tau(\epsilon) = O\left(n^7 \ln \epsilon^{-1}\right).$$

Proof. First, we compare $\mathcal{M}_C$ with $\mathcal{M}_\triangle$ using the comparison theorem (Theorem 7) to derive a bound on the mixing time of $\mathcal{M}_\triangle$ in the case of 4-connected planar triangulations. To do so we need to bound the constant A given in that theorem. Recall that A is defined as follows:

$$A = \max_{(\sigma,\tau)\in E(\mathcal{M}_\triangle)} \sum_{(X,Y)\in\Gamma(\sigma,\tau)} |\gamma_{XY}|\pi(X)P_C(X,Y)/(\pi(\sigma)P_\triangle(\sigma,\tau)),$$

where $P_\triangle$ and P_C are the transition matrices of $\mathcal{M}_\triangle$ and $\mathcal{M}_C$, respectively. Since π is the uniform distribution over $\Psi(T)$, $\pi(\sigma) = \pi(X)$ and A reduces to $\max_{(\sigma,\tau)\in E(\mathcal{M}_\triangle)} \sum_{\Gamma(\sigma,\tau)} |\gamma_{XY}| P_C(X,Y)/P_\triangle(\sigma,\tau)$. For each edge (σ,τ) in $\mathcal{M}_\triangle$ that takes a counterclockwise cycle f and makes it clockwise, $\Gamma(\sigma,\tau)$ denotes the set of edges (X,Y)

of $\mathcal{M}_C$ such that the tower $f_1, f_2, \ldots, f_k$ that takes X to Y contains the face f. Given f, the first face of the tower (f_1) uniquely determines the edge (x, y), thus $|\Gamma(\sigma, \tau)| \leq 2n + 1$. Consider any edge (X, Y) of $\mathcal{M}_C$ which reverses a tower of length k. If $k = 1$, then $P_C(X, Y) = P_\triangle(\sigma, \tau)$, since both moves happen with probability $1/2F$ where F is the number of (finite) faces. If $k \geq 2$, then $P_C(X, Y) = 1/(6kF)$. In this case $|\gamma_{XY}| = k$ and thus

$$|\gamma_{XY}| \frac{P_C(X, Y)}{P_\triangle(\sigma, \tau)} = k \frac{1/6kF}{1/2F} = \frac{1}{3}.$$

Thus in either case $|\gamma_{XY}| P_C(X, Y)/P_\triangle(\sigma, \tau) \leq 1$ and so $A \leq \max_{(\sigma,\tau)} (|\Gamma(\sigma, \tau)|) \leq 2n + 1$. Since each 3-orientation has the same stationary probability, Lemma 3(b) implies that the minimum weight of any state is $\pi_* \geq 3^{-(2n+1)}$. Therefore, by Theorems 7 and 6, the mixing time of $\mathcal{M}_\triangle$ over 4-connected planar triangulations satisfies

$$\tau(\epsilon) \leq 4 \frac{\log(\frac{1}{\epsilon \pi_*})}{\log(1/(2\epsilon))} A\tau' = O\left(\frac{\log(\frac{3^{2n+1}}{\epsilon})}{\log(1/(2\epsilon))} \, n \cdot n^5 \ln \epsilon^{-1} \right) = O(n^7 \ln \epsilon^{-1}).$$

Finally, we can extend this to non-4-connected planar triangulations, where $\mathcal{M}_\triangle$ may select nonfacial triangles. Brehm [8] proves that if T has a nonfacial triangle C, the edges on its interior that are incident to C must point towards C. This implies that for all $\sigma \in \Psi(T)$ every face on the interior of C that contains an edge of C is not bounded by a directed cycle, so they cannot be reversed, regardless of the orientation of C. Thus $\mathcal{M}_\triangle$ acts completely independently on the interior and the exterior of C.

Let T be a planar triangulation and assume that $C_1, C_2, \ldots, C_\beta$ are all the nonfacial triangles of T. Let T_i be the triangulation consisting of all faces contained within C_i and not within any other nonfacial triangle contained within C_i. Let τ_i be the mixing time of $\mathcal{M}_\triangle$ on T_i, let F_i be the number of faces within C_i, and let n_i be the number of internal vertices to T_i. Then $n = \sum_i n_i$ and the number of faces in T is $\sum_i F_i$. Therefore, by Theorem 8, the mixing time of $\mathcal{M}_\triangle$ on T will be

$$\begin{aligned} \tau(\epsilon) &\leq \max_{i=1,2,\ldots,\beta} \max \left\{ \frac{2}{p_i} \, \tau_i \left(\frac{\epsilon}{2\beta} \right), \frac{8}{p_i} \, \ln \left(\frac{\epsilon}{8\beta} \right) \right\} \\ &= \max_{i=1,2,\ldots,\beta} \max \left\{ \frac{2(2n+1)}{F_i} \, O\left(n_i^7 \ln \left(\frac{2\beta}{\epsilon} \right) \right), \frac{8(2n+1)}{F_i} \, \ln \left(\frac{\epsilon}{8\beta} \right) \right\}. \end{aligned}$$

This is maximized when $n_1 = n, \beta = 1$, and $F_1 = 2n + 1$, so

$$\tau(\epsilon) = O(n^7 \ln(\epsilon^{-1})). \qquad \square$$

In fact, this shows that $\mathcal{M}_\triangle$ is rapidly mixing on the state space $\Psi(T)$ for any planar triangulation T whose 4-connected triangulations $T_1, T_2, \ldots, T_k$ each have maximum degree (of any internal vertex) 6. Next, we use the same technique to show that $\mathcal{M}_C$ is also rapidly mixing under identical conditions.

THEOREM 10. *If T is a planar triangulation with $\Delta_I(T) \leq 6$, then the mixing time of $\mathcal{M}_C$ on the state space $\Psi(T)$ satisfies $\tau(\epsilon) = O(n^5 \ln \epsilon^{-1})$.*

Proof. The argument closely follows the proof of Theorem 9. The only difference is we do not need to apply the comparison theorem and instead can directly extend the bound on $\mathcal{M}_C$ for planar 4-connected triangulations to non-4-connected planar triangulations. $\square$

3.3. Approximate counting for maximum degree at most 6. In order to approximately count the number of 3-orientations of a planar triangulation T we design a fully polynomial randomized approximation scheme or FPRAS. In our context, an FPRAS is a randomized algorithm which, given a planar triangulation T with n internal vertices and error parameter $0 < \epsilon \leq 1$, produces a number N such that $\mathcal{P}[(1-\epsilon)N \leq |\Psi(T)| \leq (1+\epsilon)N] \geq \frac{3}{4}$, where $|\Psi(T)|$ is the number of 3-orientation of T, and runs in time polynomial in n and ϵ^{-1}. Next, we will show that such an algorithm exists.

THEOREM 11. *If T is a planar triangulation with $\Delta_I(T) \leq 6$, then there exists a FPRAS for counting the number of 3-orientations of T.*

Proof. Our proof uses similar techniques to [21]. We show how to use $\mathcal{M}_C$ to identify a vertex v_s and an orientation o_s of the edges adjacent to v_s that occurs with probability p_s. Next, we will give a procedure for creating a triangulation T_{v_s} which no longer contains v_s such that $|\Psi(T_{v_s})|$ is the number of conforming colorings in $\Psi(T)$ for which v_s has orientation o_s. Therefore, p_s is the ratio $|\Psi(T_{v_s})|/|\Psi(T)|$ and we can estimate $|\Psi(T_{v_s})|$ recursively. Thus, we estimate $|\Psi(T)|$ by approximating $|\Psi(T_{v_s})|/p_s$. Note that throughout this proof we will let the "orientation of a vertex" refer to the set of orientations of the edges adjacent to that vertex.

Let $s_{blue} = v_0, v_1, \ldots, v_x, v_{x+1} = s_{red}$ be the vertices adjacent to s_{green} and let T_{green} be the subgraph of T with vertices s_{green} and its neighbors. Without loss of generality there are two cases; s_{green} is either adjacent to one internal vertex ($x = 1$) or more than one internal vertex ($x > 1$) as shown in Figures 3.7(a) and (b), respectively. In the first case (Figure 3.7(a)), let $v_s = v_1$ be the only internal neighbor of s_{green} and let o_s be the orientation of v_s where v_s has out-degree 3 in T_{green} (in this case the only possible orientation of $v_s = v_1$). Thus, for the first case, v_s has orientation o_s with probability $p_s = 1$. Next, consider the second case where $x > 1$ (Figure 3.7(b)). Notice that in any 3-orientation of T, there must be at least one internal neighbor of s_{green} with out-degree 3 in T_{green} (i.e., in every 3-orientation, at least one of the vertices $v_1, \ldots, v_x$ has out-degree 3 in T_{green}). Theorem 9 tells us that as long as $\Delta_I(T) \leq 6$ we can efficiently approximately uniformly sample 3-orientations of T. Sample conforming colorings to approximate the probability p_i that for a random sample from Ω, v_i has out-degree 3 in T_{green} for all vertices $v_i \in \{v_1, \ldots, v_x\}$. Let v_s be the internal vertex $v_i \in \{v_1, \ldots, v_x\}$ with the highest probability p_i and o_s be the orientation of v_s where v_s has out-degree 3 in T_{green}. Thus, for the second case, v_s has orientation o_s with probability $p_s = \max\{p_1, \ldots, p_x\}$. Note that in either case $p_s = \Omega(n^{-1})$.

Next, for both cases, we will give a procedure for creating a triangulation T_{v_s} which no longer contains v_s such that $|\Psi(T_{v_s})|$ is the number of conforming colorings in $\Psi(T)$ for which v_s has out-degree 3 in T_{green} (i.e., v_s has orientation o_s).

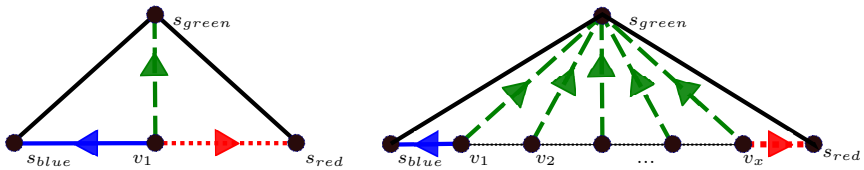

FIG. 3.7. *The two cases for the subgraph T_{green}.*

In any 3-orientation of T where v_s has out-degree 3 in T_{green}, all other edges adjacent to v_s must be incoming. Thus, v_s must look as shown in Figure 3.8(a). Note that the number of incoming green edges to vertex v_s can vary. Additionally, v_{s-1} might be s_{blue} and v_{s+1} might be s_{red}. For example, if $x = 1$ (the first case, Figure 3.7(a)), then $v_{s-1} = s_{blue}$ and $v_{s+1} = s_{red}$. For each edge (u, v_s) adjacent to v_s such that $u \neq v_{s-1}, v_{s+1}$ replace (u, v_s) with a new edge (u, s_{green}). Next, delete v_s and all edges incident to v_s as shown in Figure 3.8(b). Notice that we now have a new triangulation, T_{v_s} with one less vertex and each 3-orientation of T where v_s has out-degree 3 in T_{green} corresponds bijectively with a 3-orientation of T_{v_s}. Additionally, we have not increased the degree of any vertex except for the external vertex s_{green} so if $\Delta_I(T) \leq 6$, then $\Delta_I(T_{v_s}) \leq 6$). This is essential to allowing the Markov chain to be used recursively. Therefore, p_s is the ratio $|\Psi(T_{v_i})|/|\Psi(T)|$ and we can estimate $|\Psi(T_{v_s})|$ recursively. Thus, we estimate $|\Psi(T)|$ by approximating $|\Psi(T_{v_s})|/p_s$. It follows from [21] and Theorem 9 that this procedure gives us a FPRAS. ∎

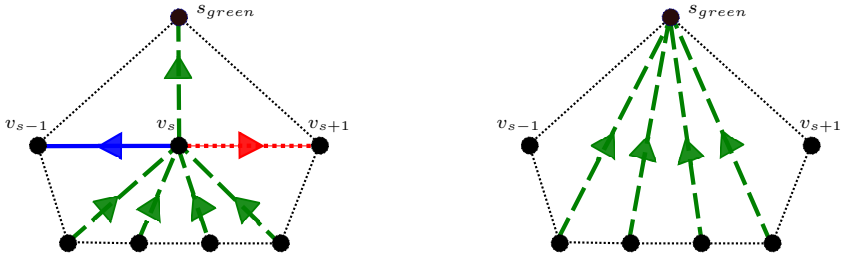

FIG. 3.8. *How to remove the vertex v_s.*

3.4. Slow mixing of $\mathcal{M}_\triangle$ for unbounded degree. We now exhibit a triangulation on which $\mathcal{M}_\triangle$ takes exponential time to converge. A key tool is *conductance*, which for an ergodic Markov chain $\mathcal{M}$ with distribution π and transition matrix $\mathcal{P}$ is

$$\Phi_{\mathcal{M}} = \min_{\substack{S \subseteq \Psi \\ \pi(S) \leq 1/2}} \sum_{s_1 \in S, s_2 \in \overline{S}} \pi(s_1)\mathcal{P}(s_1, s_2)/\pi(S).$$

The following theorem relates the conductance and mixing time (see [19]).

THEOREM 12. *For any Markov chain $\mathcal{M}$ with conductance $\Phi_{\mathcal{M}}$, the mixing time of the Markov chain $\mathcal{M}$ on the state space Ψ satisfies*

$$\tau(\epsilon) \geq \left(\frac{1}{4\Phi_{\mathcal{M}}} - \frac{1}{2}\right) \log\left(\frac{1}{2\epsilon}\right).$$

We show that for the generalized triangulation G given in Figure 3.9 with $n = 4t - 2$ internal vertices, $\mathcal{M}_\triangle$ takes exponential time to converge. Specifically, we show that although there is an exponential number of 3-orientations where the edge (v_0, v_{t+1}) is colored blue or red, all paths between these 3-orientations with (v_0, v_{t+1}) colored differently must include a 3-orientation where (v_0, v_{t+1}) is colored green. There is only a single 3-orientation that satisfies this property (namely, the one pictured in Figure 3.9), which creates a bottleneck in the state space.

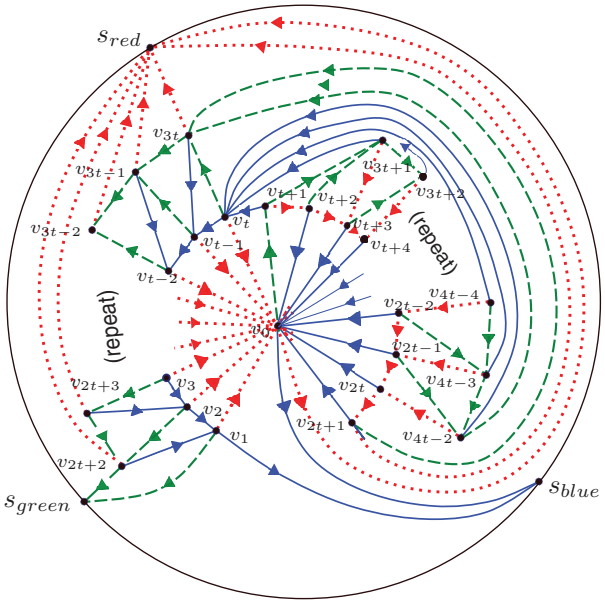

FIG. 3.9. *A triangulation for which $\mathcal{M}_\triangle$ mixes slowly.*

THEOREM 13. *For any (large) n, there exists a triangulation T of size n for which the mixing time of the Markov chain $\mathcal{M}_\triangle$ on the state space $\Psi(T)$ satisfies*

$$\tau(\epsilon) = \Omega(2^{n/4} \ln \epsilon^{-1}).$$

Proof. Let D be the set of 3-orientations of G with (v_0, v_{t+1}) colored red or green and $\overline{D}$, the complement of D, be the set of 3-orientations with (v_0, v_{t+1}) colored blue. In order to show that both D and $\overline{D}$ are exponentially large we produce a triangulation in each set which contains roughly t directed triangles which do not share any edges and reversing these triangles does not change the colors of the edges adjacent to v_0. Hence each of the 2^t choices of the orientations of these triangles gives a distinct 3-orientation with edge (v_0, v_{t+1}) colored appropriately.

First, consider the 3-orientation in Figure 3.10 which is in D. Notice that triangles $T_1, T_2, \ldots, T_{t-2}$ do not share any edges and reversing these triangles does not change the color of any edges adjacent to v_0. Each of these triangles has two possible orientations and each of these 2^{t-2} choices of the orientations of the triangles gives a distinct 3-orientation with edge (v_0, v_{t+1}) colored red implying that

$$|D| \geq 2^{t-2} = 2^{(n-6)/4}. \tag{3.1}$$

Next, consider the coloring in Figure 3.11. Notice that triangles $S_1, S_2, \ldots, S_{t-1}$ do not share any edges and reversing these triangles does not change the color of any edges adjacent to v_0. Each of these triangles has two possible orientations and each of these 2^{t-1} choices of the orientations of the triangles gives a distinct 3-orientation with edge (v_0, v_{t+1}) colored blue implying that

$$|\overline{D}| \geq 2^{t-1} = 2^{(n-2)/4}. \tag{3.2}$$

Next, we show that there is only one 3-orientation of G with (v_0, v_{t+1}) colored green, corresponding to Figure 3.9. By the vertex condition, if edge (v_0, v_{t+1}) is green

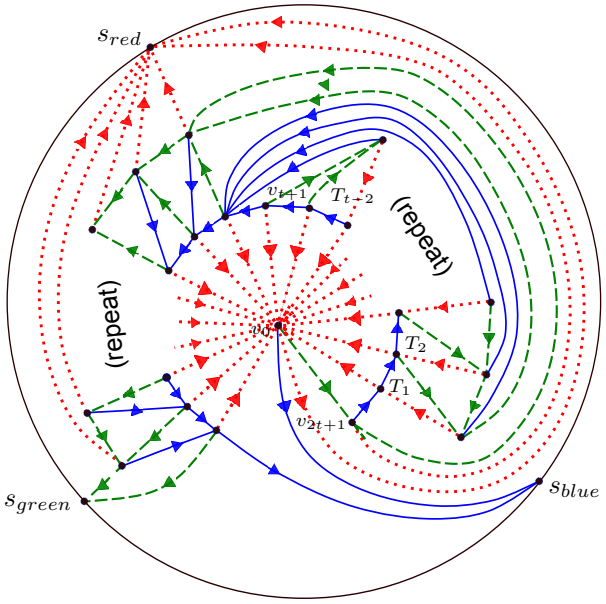

FIG. 3.10. *There is an exponential number of* 3*-orientations with edge* (v_0, v_{t+1}) *colored red corresponding to the different orientations of triangles* $T_1, T_2, \ldots, T_{t-2}$.

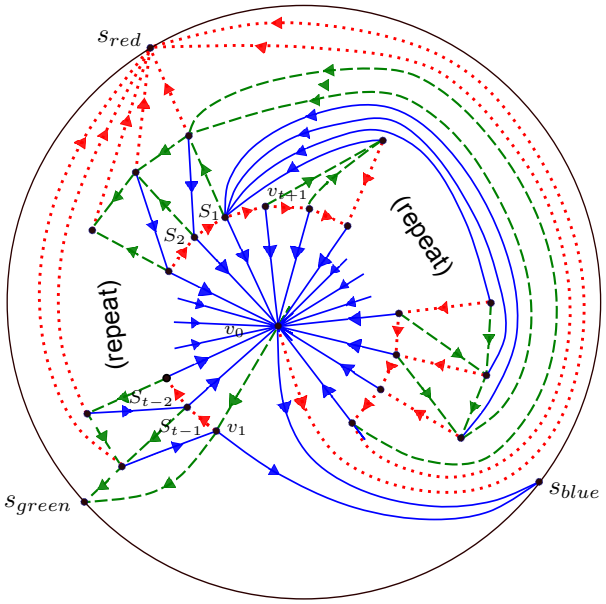

FIG. 3.11. *There is an exponential number of* 3*-orientations with edge* (v_0, v_{t+1}) *colored blue corresponding to the different orientations of triangles* $S_1, S_2, \ldots, S_{t-2}$.

then edges $(v_0, v_1), (v_0, v_2), \ldots, (v_0, v_t)$ must all be directed toward v_0 and colored red; this is because the edge (v_0, s_{blue}) is blue and directed towards s_{blue} in every 3-orientation of G. Similarly, edges $(v_0, v_{t+2}), (v_0, v_{t+3}), \ldots, (v_0, v_{2t+1})$ must all be blue and directed toward v_0. Since v_{t+1} has degree 4 and has the incoming green

edge (v_0, v_{t+1}), the other edges incident to v_{t+1} are determined; (v_{t+1}, v_t) is blue, (v_{t+1}, v_{3t+1}) is green, and (v_{t+1}, v_{t+2}) is red all directed away from v_{t+1}. Knowing the colors and direction of the edges incident to v_0 and v_{t+1} forces the color and direction of the edges incident to v_{t+2}. Similarly, v_{t+1} and v_{t+2} force v_{3t+1} and v_0, v_{t+2} and v_{3t+1} force v_{t+3} and so on until the color and direction of all edges incident to vertices $v_{t+1}, v_{t+2}, \ldots, v_{2t+1}$ and $v_{3t+1}, v_{3t+2}, \ldots, v_{4t-2}$ are forced. Next, consider v_t; we know the edges $(v_t, v_{t+1}), (v_t, v_{3t+1}), (v_t, v_{3t+2}), \ldots, (v_t, v_{4t-2})$ are all blue and directed toward v_t which implies (v_t, v_{3t}) and (v_t, v_{t-1}) must be directed outward and green and blue, respectively. Now consider v_{3t}; we have already shown that all edges incident to v_{3t} except for $(v_{3t}, v_{t-1}), (v_{3t}, v_{3t-1}), (v_{3t}, v_{s_{red}})$ have a forced color and are directed inward. Thus, these 3 edges must all be directed outwards with colors blue, green, and, red respectively. Similarly, knowing the colors and directions of all edges incident to v_{3t}, v_t and v_0 forces the colors and directions of edges incident to v_{t-1} and v_{3t}, v_{t-1} forces v_{3t-1} and so on for the remaining vertices. Since all the edge colors and orientations are fixed, this implies there is a unique 3-orientation with (v_0, v_{t+1}) colored green. To go from a configuration where edge (v_0, v_{t+1}) has color red (blue) to blue (resp., red) one must go through a coloring where the edge is green. This is because the only choices for edge (v_0, v_{t+1}) are red directed toward v_0, blue directed toward v_0, and green directed away, and any move that changes the color must also change the direction. This is due to the fact that the Markov chain reverses the direction of the edges of a triangle and does not affect any other edges. Therefore, if a move changes the color of an edge this implies that the edge is on the triangle being reversed and thus the direction of the edge must also change.

Finally, given the bounds on $|D|$ and $|\overline{D}|$, we derive a bound on the mixing time of $\mathcal{M}_\triangle$. Let g be the single 3-orientation which has edge (v_0, v_{t+1}) colored green. If $\pi(D) \leq 1/2$, then combining the definition of conductance with the bound on $|D|$ yields

$$\begin{aligned}
\Phi_{\mathcal{M}_\triangle} &\leq \frac{1}{\pi(D)} \sum_{d_1 \in D, d_2 \in \overline{D}} \pi(d_1)\mathcal{P}(d_1, d_2) \\
&= \frac{1}{\pi(D)} \sum_{d_2 \in \overline{D}} \pi(g)\mathcal{P}(g, d_2) \\
&\leq \frac{\pi(g)}{\pi(D)} \leq \frac{1/Z}{2^{(n-6)/4}/Z} = \frac{1}{2^{(n-6)/4}}.
\end{aligned}$$

If $\pi(D) > 1/2$, then $\pi(\overline{D}) \leq 1/2$ and so by detailed balance and the bound on $|\overline{D}|$,

$$\begin{aligned}
\Phi_{\mathcal{M}_\triangle} &\leq \frac{1}{\pi(\overline{D})} \sum_{d_1 \in \overline{D}, d_2 \in D} \pi(d_1)\mathcal{P}(d_1, d_2) \\
&= \frac{1}{\pi(\overline{D})} \sum_{d_1 \in \overline{D}} \pi(d_1)\mathcal{P}(d_1, g) \\
&= \frac{1}{\pi(\overline{D})} \sum_{d_1 \in \overline{D}} \pi(g)\mathcal{P}(g, d_1) \\
&\leq \frac{\pi(g)}{\pi(\overline{D})} \leq \frac{1/Z}{2^{(n-2)/4}/Z} = \frac{1}{2^{(n-2)/4}}.
\end{aligned}$$

In both cases, $\Phi_{\mathcal{M}_\triangle} \leq 2^{-(n-6)/4}$. Applying Theorem 12 proves that the mixing time

of $\mathcal{M}_\triangle$ satisfies

$$\tau(\epsilon) \geq \left(2^{(n-14)/4} - \frac{1}{2}\right) \log\left(\frac{1}{2\epsilon}\right) = \Omega(2^{n/4} \ln \epsilon^{-1}). \qquad \square$$

Remark 1. Combining this result with the comparison argument in section 3.2 shows that $\mathcal{M}_C$ can also take exponential time to converge.

4. Sampling the 3-orientations of triangulations on n internal vertices. We consider a local "edge-flipping" Markov chain $\mathcal{M}_E$ for sampling uniformly from Ψ_n and show $\mathcal{M}_E$ is always rapidly mixing. Our argument relies on a bijection with pairs of Dyck paths to relate the mixing time of a chain on Dyck paths to $\mathcal{M}_E$ using the comparison method [11, 27]. Define $\mathcal{M}_E$ as follows (see Figure 4.1).

The Markov chain $\mathcal{M}_E$

Starting at any $\sigma_0 \in \Psi_n$, iterate the following:

- Choose facial triangles T_1 and T_2 with shared edge $\overrightarrow{xy}$ uniformly at random.
- Pick a vertex $z \in T_1 \cup T_2$ with $z \neq x, y$ uniformly at random.
- If the edge (z, x) is directed $\overrightarrow{zx}$, then with probability $1/2$ replace the path $\{\overrightarrow{zx}, \overrightarrow{xy}\}$ by the path $\{\overrightarrow{xz}, \overrightarrow{zw}\}$ where w is the remaining vertex of $T_1 \cup T_2$.
- Otherwise, $\sigma_{i+1} = \sigma_i$.

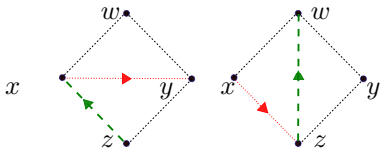

FIG. 4.1. *A move of $\mathcal{M}_E$ (a red/green swap).*

If the edge $\overrightarrow{zx}$ with color c_i is replaced by the edge $\overrightarrow{xz}$ with color c_j, we call this a c_i/c_j *swap* (see, e.g., Figure 4.1). Bonichon, Le Saëc, and Mosbah showed in [6] that $\mathcal{M}_E$ connects the state space Ψ_n. Since all valid moves have the same transition probabilities, we can conclude that $\mathcal{M}_E$ converges to the uniform distribution over state space Ψ_n (see, e.g., [30]).

4.1. The bijection between Ψ_n and pairs of Dyck paths. The key to bounding the mixing time of $\mathcal{M}_E$ is a bijection between Ψ_n and pairs of nonoverlapping Dyck paths of length $2n$, introduced by Bonichon [5]. Dyck paths can be thought of as strings $a_1 a_2, \ldots, a_{2n}$ containing an equal number of 1's and -1's, where for any $1 \leq k \leq 2n$, $\sum_{i=1}^{k} a_i \geq 0$. Recall that a 3-orientation of a triangulation can be viewed as a union of three trees, one in each color. In the bijection, the bottom Dyck path corresponds to the blue tree, and the top Dyck path indicates the degree of each vertex in the red tree. The green tree is determined uniquely by the blue and red trees. More specifically, given $\sigma \in \Psi_n$, to determine the bottom Dyck path, start at the root of the blue tree and trace along the border of the tree in a clockwise direction until you end at the root. The first time you encounter a vertex, insert a 1 in the Dyck path, the second time you encounter the vertex insert a -1. Let $v_1, v_2, \ldots, v_n$ be the order of the vertices as they are encountered by performing this depth first search (DFS) traversal of the blue tree in a clockwise direction and define L to be

the resulting linear order on the vertices. Let d_i be number of incoming red edges incident to v_i. Notice that since v_1 is adjacent to s_{blue} and s_{green}, $d_1 = 0$. Let r be the number of incoming red edges incident to s_{red}. The top Dyck path is as follows: $1(-1)^{d_2}1(-1)^{d_3}1(-1)^{d_4}, \ldots, 1(-1)^{d_n}1(-1)^{r}$. The structure of the 3-orientation guarantees that the top path will never cross below the bottom path. Figure 4.2 gives an example. See [5] for more details and a complete proof that this is a bijection.

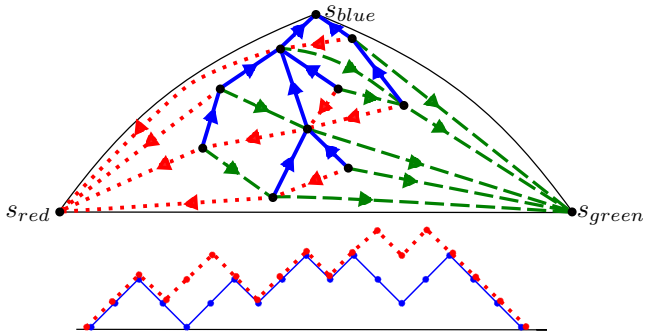

FIG. 4.2. *The bijection between Ψ_n and pairs of Dyck paths.*

We bound the mixing time of $\mathcal{M}_E$ by comparing it to $\mathcal{M}_D$, an efficient Markov chain on (pairs of) Dyck paths introduced by Luby, Randall, and Sinclair [23]. The algorithm proceeds as follows. At each step select a point on one of the two Dyck paths uniformly at random. If the point is a local maximum (or minimum), then push it down (or up) with probability 1/2 as shown in Figure 4.3(a–b). If this move is blocked by a local maximum (or minimum) in the bottom (or top) Dyck path as shown in Figure 4.3(c), then push both Dyck paths down (or up) with probability 1/2 as shown in Figure 4.3(c–d). The following theorem due to Wilson [31] bounds the mixing time of $\mathcal{M}_D$.

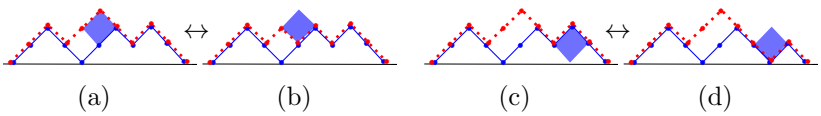

FIG. 4.3. *Two moves of the Markov chain $\mathcal{M}_D$.*

THEOREM 14 (Wilson). *The mixing time of $\mathcal{M}_D$ on state space Ψ_n satisfies*

$$\tau(\epsilon) = \Theta(n^3 \log(n/\epsilon)).$$

Using the above bijection, the Markov chain $\mathcal{M}_D$ on Dyck paths can be translated into a Markov chain on 3-orientations of triangulations, but its moves are quite unnatural in that setting. We obtain a bound on the mixing time of $\mathcal{M}_E$ using Theorem 14 together with a careful comparison argument.

4.2. Fast mixing of $\mathcal{M}_E$. Next, we show that $\mathcal{M}_E$ is efficient for sampling from Ψ_n by comparing $\mathcal{M}_E$ and $\mathcal{M}_D$ using the comparison theorem (Theorem 7) introduced in section 3.2. First, we introduce some notation. Let c_1 be blue, let c_2 be red, and let c_3 be green. Given a vertex v and $i \in \{1, 2, 3\}$, the unique outgoing edge of v with color c_i is called v*'s* c_i *edge*. We also define the *first* (*last*) incoming c_i-edge of v to be the incoming c_i-edge of v that is in a facial triangle with v's c_{i-1}

edge (resp., v's c_{i+1} edge, where the subscripts are taken modulo 3). In our canonical paths, we will often need to move a c_j edge, say $\overrightarrow{vx}$, from some neighbor x of v to another neighbor y of v across several c_i edges. This is achieved through a *sequence of c_j/c_i swaps* as in Figure 4.4.

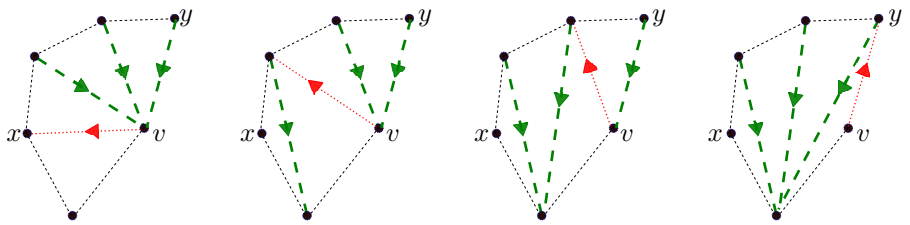

FIG. 4.4. *A sequence of red/green swaps.*

Throughout the proof the vertex numbering we use refers to L the ordering of the vertices given by a DFS traversal of the blue tree in the clockwise direction as defined in section 4.1. We also point out that given this ordering, any red edge $\overrightarrow{v_iv_j}$ satisfies $i < j$. For green edges the opposite is true thus any green edge $\overrightarrow{v_iv_j}$ satisfies $j < i$. See [5] for details.

We are now ready to bound the mixing time of $\mathcal{M}_E$.

THEOREM 15. *The mixing time of $\mathcal{M}_E$ on the state space Ψ_n satisfies*

$$\tau(\epsilon) = O(n^8 \log(n/\epsilon)).$$

Proof. In order to apply the comparison theorem (Theorem 7) to relate the mixing time of $\mathcal{M}_E$ with the mixing time of $\mathcal{M}_D$ we need to define, for each transition of $\mathcal{M}_D$, a canonical path using transitions of $\mathcal{M}_E$. Then we will bound the number of canonical paths that use each edge of $\mathcal{M}_E$. There are several cases to consider; depending on whether a move affects the top path, the bottom path, or both and whether it inverts a valley or a peak. If the move $e = (X, Y)$ affects both paths, we view the move as two separate moves (X, Z) and (Z, Y), one on each path, and we concatenate the canonical paths as follows: $\gamma_{X,Y} = (\gamma_{X,Z}, \gamma_{Z,Y})$. Hence in the following, we assume that the transitions of $\mathcal{M}_D$ affect only one Dyck path.

A peak to valley move on the top Dyck path. Let $e = (X, Y)$ be a transition of $\mathcal{M}_D$ that inverts a peak on the top Dyck path. Suppose e moves the ith 1 (where $i > 1$) on the top path to the right one position (i.e., the Dyck path move swaps the ith 1 with a -1 on its right, inverting a peak). From the bijection, we know this move does not affect the blue tree and corresponds to, in the red tree, increasing the incoming degree of v_i by one and decreasing the incoming degree of v_{i+1} by one. Recall that the vertex numbering corresponds to the ordering of the vertices given by a DFS traversal of the blue tree in the clockwise direction as defined in section 4.1. If v_i and v_{i+1} are adjacent in the blue tree (there is a blue edge $\overrightarrow{v_{i+1}v_i}$), this implies that there is a red/green swap involving v_i's green edge and v_{i+1}'s first incoming red edge. This swap exists because the vertex order comes from the clockwise order of the vertices in the blue tree which implies v_i has no incoming blue edges between $\overrightarrow{v_{i+1}v_i}$) and v_i's green edge. Additionally, we know that v_{i+1} has at least one incoming red edge so these three edges, $\overrightarrow{v_{i+1}v_i}$, v_i's green edge, and v_{i+1}'s first incoming red edge must form a cycle. See Figure 4.5 for an example. This swap is exactly the peak to valley move, so $\gamma_{XY} = e$.

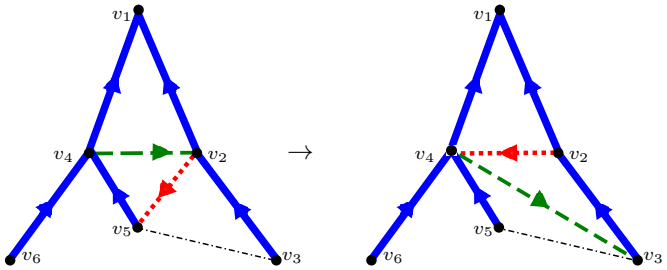

FIG. 4.5. *A red/green swap involving v_4's green edge and v_5's first incoming red edge. Notice that this swap increase does not affect the blue tree and in the red tree increases the incoming degree of v_4 by one and decreases the incoming degree of v_5 by one.*

Otherwise, we define two stages in the canonical path γ_{XY}. To assist in defining the canonical paths, let v_g be the parent of v_i in the green tree. Lemma 16, whose proof we defer to the end of the section, states that v_g is not s_{green}. Let v_j be the parent of v_g in the red tree. Notice that $i < j$, since $j > g$ (because $\overrightarrow{v_g v_j}$ is an edge in the red tree) and v_i's green edge prevent v_j from satisfying $i \geq j > g$ as shown in Figure 4.6.

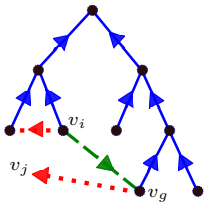

FIG. 4.6. *The vertex v_i's red and green edges prevent v_j from satisfying $i \geq j > g$.*

Stage 1. In the first stage of the path γ_{XY} we make the sequence of red/green swaps centered at v_g that move the red edge $\overrightarrow{v_g v_j}$ to $\overrightarrow{v_g v_i}$ without affecting any other red edges as shown in Figure 4.7, step 1 (see Figure 4.4 for details on the sequence of swaps). Note that if $j = i + 1$, then we are done and Stage 2 is skipped.

Stage 2. In the second stage we transfer an incoming red edge from v_{i+1} to v_j, completing $\gamma_{X,Y}$. Recall that $j > i + 1$, so we do this iteratively by moving an incoming red edge $\overrightarrow{yx}$ either to one of x's neighbors in the blue tree that is larger in L or to x's parent in the red tree, which is also larger in L, if it is a leaf and has no neighbors as shown in Figure 4.7, steps 2 and 3. We claim it is always possible to make one of these moves. If x has a neighbor y in the blue tree such that $L(y) = L(x) + 1$, then there must be a green/red swap centered at x and involving x's green edge that moves an incoming red edge from x to y as desired. Next, if x is a leaf with red edge $\overrightarrow{xr_x}$, then again there is a green/red swap centered at x involving x's green edges that moves an incoming red edge from x to r_x as desired. Finally, notice that using this canonical path we never bypass v_j because the original red edge $\overrightarrow{v_g v_j}$ blocked any blue leaves between v_{i+1} and v_g from having red parents higher in L than v_j.

Given a transition (Z, W) of $\mathcal{M}_E$ we must bound the number of canonical paths γ_{XY} using this edge. To do so, we analyze the amount of information needed in addition to (Z, W) to determine X and Y uniquely. We record the vertex v_i and the vertex v_j. If v_i and v_{i+1} are adjacent, we record v_{i+1} instead of v_j. Notice in this case the canonical path only involves red/green and green/red swaps. If we are moving a

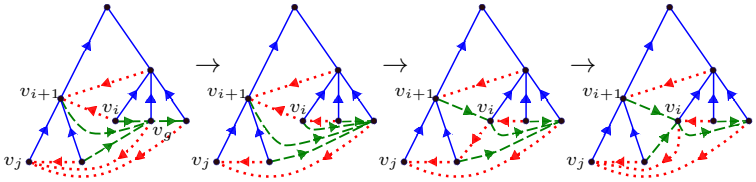

FIG. 4.7. *The canonical path to invert a peak on the top Dyck path.*

red edge to a higher vertex in L, then we are in stage 2 and otherwise we are in stage 1. Given this information we can uniquely recover X and Y. We need only record two vertices, so in this case there are at most n^2 canonical paths which use any edge (Z, W).

A valley to peak move on the top Dyck path. Consider the case where $e = (X, Y)$ inverts a valley on the top Dyck path. Recall that the chain $\mathcal{M}_D$ is reversible, so there is an edge $e' = (Y, X)$ which inverts a peak on the top Dyck path. We will define the canonical path from X to Y to be the reverse of the canonical path from Y to X which was defined explicitly in the previous case. Note that canonical paths are defined in a specific way, so it is not always the case that the reverse of the canonical path from X to Y is the canonical path from Y to X. Consider the canonical path $\gamma_{YX} = (Y = X_0, X_1, \ldots, X_k = X)$ defined in the peak to valley case above. Let $\gamma_{XY} = X_k = X, X_{k-1}, \ldots, X_1, X_0 = Y$ be the path γ_{YX} reversed. Since γ_{YX} is a valid path, $P(X_i, X_{i+1}) > 0$ for $(0 \leq i < k)$. The chain $\mathcal{M}_E$ is reversible thus implying $P(X_{i+1}, X_i) > 0$ for $(0 \leq i < k)$. Rewriting the previous expression slightly gives the equivalent statement $P(X_i, X_{i-1}) > 0$ for $(k \geq i > 0)$ and thus γ_{XY} is a valid path. Given a transition (Z, W) of $\mathcal{M}_E$ it remains to bound the number of canonical paths γ_{XY} using this edge in this case. For any canonical path γ_{XY} that inverts a valley on the top Dyck path and uses edge (Z, W) by the definition of the path, there exists a canonical path $\gamma_{Y,X}$ that inverts a peak on the top Dyck path and uses edge (W, Z). From the previous argument for the peak to valley case, there are at most n^2 canonical paths $\gamma_{Y,X}$ which invert a peak on the top Dyck path and use edge (W, Z) and thus there are at most n^2 canonical paths $\gamma_{X,Y}$ which invert a valley on the top Dyck path and use edge (Z, W).

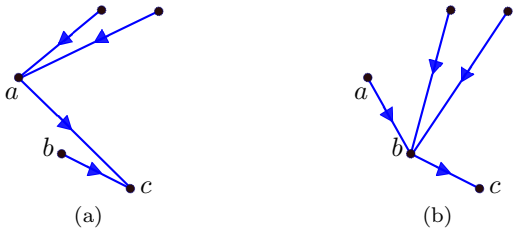

FIG. 4.8. *A transition of $\mathcal{M}_D$ that inverts a valley on the bottom Dyck path takes the blue tree from* (a) *to* (b).

A valley to peak move on the bottom Dyck path. Next, consider the case where $e = (X, Y)$ inverts a valley on the bottom Dyck path. This affects the blue tree as follows (see Figure 4.8): a's blue edge moves from c to b, and all the (blue) children of $\overrightarrow{ac}$ (if any exist) become children of $\overrightarrow{bc}$. See Figure 4.9 for an example that

shows a Dyck path move on the bottom path and the corresponding effect on the 3-orientation. However, to define the canonical path between these two configurations, it is necessary to also know what the top Dyck path looks like, as it determines the red (and therefore the green) tree. Figure 4.10 shows how the red and green tree might look. Our path will first update the blue tree from X to match the blue tree of Y, and then update the red tree (and therefore the green tree) to match the red tree of Y using the steps outlined in the previous two cases. For a vertex $v \in T$ let r_v denote the head of v's red edge in X. We will go through four distinct stages in the canonical path. In stage 1 the blue edge of a moves from c to b. Then in stage 2, a's red edge moves into position for stage 3, where all incoming blue edges to a move down to point to b. Finally, in stage 4 we repair the red tree.

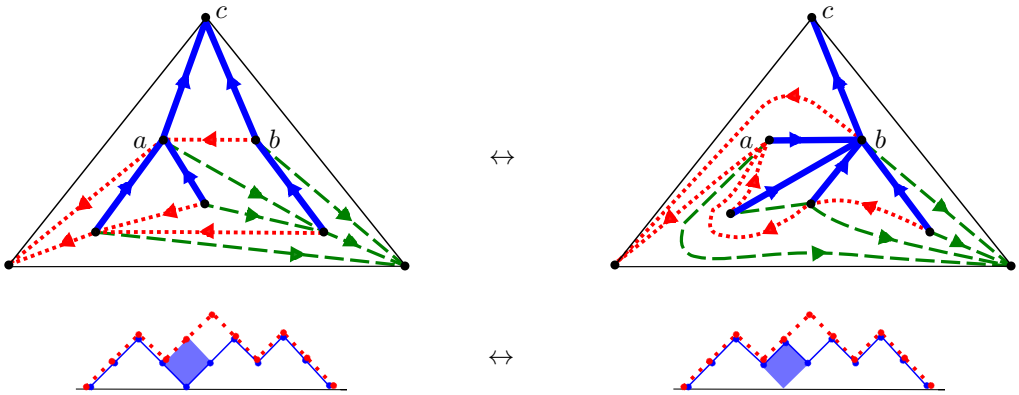

FIG. 4.9. *A transition of $\mathcal{M}_D$ that inverts a valley to a peak on the bottom Dyck path.*

Stage 1. Given the vertex condition (Figure 2.1a) for b and the bijection between the bottom Dyck path and the blue tree, there is no edge in the angle $\angle acb$ and thus a, b, and c form a triangle in our triangulation. Vertex b may have some green edges coming in between its blue edge $\overrightarrow{bc}$ and its red edge $\overrightarrow{br_b}$. If so, then $\overrightarrow{ab}$ is an edge, as in Figure 4.10(a). If not, then we can skip the first step and go directly to Figure 4.10(b). The first step along the canonical path from X to Y is to rotate b's red edge to point to a (see Figure 4.10(a–b)). This is accomplished through a sequence of red/green swaps, one for each green edge coming into b, as in Figure 4.4. Now we are ready to move the blue edge $\overrightarrow{ac}$ to $\overrightarrow{ab}$ by swapping with b's red edge, as in Figure 4.10(b–c).

Stage 2. Consider vertex a. Counterclockwise from a's blue edge, there may be some green edges coming into a, followed by the red edge $\overrightarrow{ar_a}$. If there are green edges, let d be the tail of the last incoming green edge to a; however, if there are no green edges, then $r_a = d$. In this stage of our canonical path, a's red edge moves from r_a to d (if $r_a \neq d$) by a series of red/green swaps. See Figure 4.4(c–d).

Stage 3. Next, we use a's red edge to move all the blue children of $\overrightarrow{ab}$ to point to b, one at a time, in a clockwise manner. See Figure 4.4(d–e). Now the blue tree is completely fixed.

Stage 4. Finally, we must repair the red tree. Notice that the red edges of a and b are the only red edges that we moved; we must move them to their proper place. We must increase the degree of r_b and r_a back to match their in-degree in X. To do this without affecting the blue tree, we first make a's red edge point to r_b (we'll call this *Stage* 4*a*) and then make b's red edge point to r_a (*Stage* 4*b*). These moves can each be accomplished by a sequence of red/green swaps without affecting the blue tree.

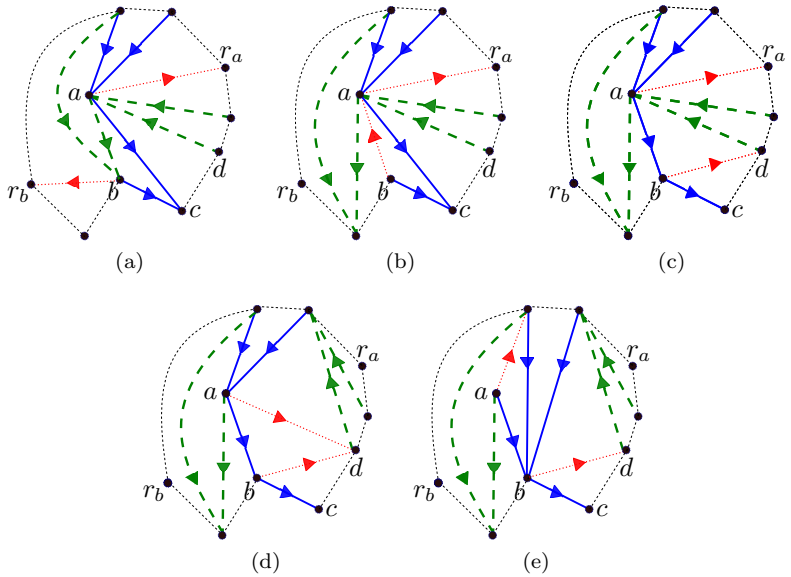

FIG. 4.10. *The canonical path to invert a valley on the bottom Dyck path.*

Given a transition (Z, W) of $\mathcal{M}_E$, we must upper bound the number of canonical paths $\gamma_{X,Y}$ that use this edge. If (Z, W) is in stage 1, we need to remember vertices a and r_b, and a bit to tell us whether or not we have moved $\overrightarrow{ac}$ yet. Given this information, we can recover b and c and can undo all red/green swaps in order to get back to X. Given X we can find Y since we know which valley to flip up. If (Z, W) is in stage 2, then we need only record r_b, since (Z, W) moves a's red edge, so we know a. To get back to the last configuration in stage 1, we just need to move a's red edge counterclockwise until it can't make any more red/green swaps. Thus we can get back to the last configuration in stage 1, and using a and r_b we can recover X. If (Z, W) is in stage 3, we need to record r_b. Each move in stage 3 takes a child of $\overrightarrow{ab}$ and moves it to point to b. Hence, we know a. Notice that since $\triangle abc$ was facial in X, all blue edges coming into b in σ_1 before $\overrightarrow{ab}$ (in the counterclockwise direction) were children of $\overrightarrow{ac}$ in X. Thus, given a, we know that we must use a's red edge to move each of these children back up to a. This brings us back to the last configuration in stage 2; using a and r_b, we can recover X. If (Z, W) is in stage 4a, then we know that the blue tree agrees with Y, and the red edges of a and b are the only red edges in a different position in Z than in Y. Since (Z, W) moves a's red edge, we know a, and b is the vertex that shares a's blue edge. Given b, it is easy to recover r_a, since to find r_a, just move b's red edge counterclockwise until it can't make any more red/green swaps. We need to record r_b and then it is easy to get to Y. If (Z, W) is in stage 4b, then we know that the blue tree agrees with Y and b's red edge is the only red edge that is in a different position in Z than in Y. Since (Z, W) moves b's red edge, we know b. As described in stage 4a, it is easy to then find r_a; move b's red edge all the way there to get to Y. In each of the four stages we need to record a maximum of two vertices and a single bit. This implies that in this case there are $O(n^2)$ canonical paths which use any edge (Z, W).

A peak to valley move on the bottom Dyck path. Finally, consider the

case where $e = (X, Y)$ inverts a peak on the bottom Dyck path. Recall that the chain $\mathcal{M}_D$ is reversible, so there is an edge $e' = (Y, X)$ which inverts a valley on the bottom Dyck path. We will define the canonical path from X to Y to be the reverse of the canonical path from Y to X. Let $\gamma_{YX} = (Y = X_0, X_1, \ldots, X_k = X)$ be the canonical path from Y to X, then $\gamma_{XY} = X_k = X, X_{k-1}, \ldots, X_1, X_0 = Y$ is the path γ_{YX} reversed. As in the valley to peak on the top Dyck Path case, it is easily shown due to the reversibility of $\mathcal{M}_E$ that γ_{XY} is a valid path. Similarly, given a transition (Z, W) there are $O(n^2)$ canonical paths which invert a valley on the bottom path and use edge (Z, W) and thus there are $O(n^2)$ canonical paths $\gamma_{X,Y}$ which invert a peak on the bottom path and use edge (W, Z).

We have shown that in each of the four cases above there is a maximum of $O(n^2)$ canonical paths which use any edge (Z, W). If the move of $\mathcal{M}_D$ affects both the top and bottom paths, we can think of this move as two moves, each of which affects only the top or bottom path; hence, we concatenate the paths for each of those moves. Therefore, if we record a bit to decide if the move of $\mathcal{M}_D$ affects both the top and bottom paths, as well as two bits to decide which of the cases we are in, this implies that across all cases there is a maximum of $O(n^2)$ canonical paths which use any edge (Z, W). Notice that the maximum length of any path γ_{XY} is $O(n^2)$. We can now upper bound the quantity A which is needed to apply comparison theorem (Theorem 7) as follows:

$$\begin{aligned} A &= \max_{(Z,W)\in E(P)} \left\{ \frac{1}{\pi(Z)P(Z,W)} \sum_{\Gamma(Z,W)} |\gamma_{XY}|\pi(X)P'(X,Y) \right\} \\ &\leq \max_{(Z,W)\in E(P)} \left\{ 4n \sum_{\Gamma(Z,W)} \frac{O(n^2)}{2n} \right\} \leq O(n^4). \end{aligned}$$

Moreover, we can bound π_* as follows:

$$\pi_* = \min_{X\in\Psi} \pi(X) = \frac{1}{C_{n+2}C_n - C_{n+1}^2} \geq \frac{1}{30^n}.$$

Applying Theorems 14 and 7, we get the following:

$$\begin{aligned} \tau(\epsilon) &= O\left(\frac{\log(\frac{1}{\epsilon\pi_*})}{\log(1/(2\epsilon))} n^4 \cdot n^3 \log(n/\epsilon) \right) \\ &= O\left(\frac{n\log 30 - \log\epsilon}{-\log(2\epsilon)} n^7 \log(n/\epsilon) \right) \\ &= O\left(n^8 \log(n/\epsilon) \right). \end{aligned}$$

Therefore, $\mathcal{M}_E$ is an efficient sampling algorithm for sampling from the set of all 3-orientations over any triangulation on n internal vertices. ∎

Finally, we will prove Lemma 16 which was used in the definition of the canonical path for a valley to peak move on the top Dyck path. Although this proof is not complex, it relies heavily on properties of Schnyder woods proven in [5].

LEMMA 16. *Let $e = (X, Y)$ be a transition of $\mathcal{M}_D$ that moves the i*th 1 *(where $i > 1$) on the top path to the right one position. Then the parent of v_i in the green tree is not s_{green}.*

Proof. Let v_g be the parent of v_i in the green tree. We will show that v_g is not s_{green}; that is, v_i cannot have its green edge point to s_{green} as long as $e = (X, Y)$ is a valid transition of $\mathcal{M}_D$. For the sake of contradiction, suppose $\overrightarrow{v_i s_{green}}$ is an edge in X. Let P be the path from s_{blue} to v_i in the blue tree combined with the edge $\overrightarrow{v_i s_{green}}$. We will use this path to partition the vertices of X into two sets according to which side of the path they are on: let S be the set of vertices on the same side of P as v_{i+1} (not including the vertices along P), and let $\overline{S}$ be the remaining vertices. For any triangulation $Z \in \Psi_n$ let $R_Z(S)$ be the total number of incoming red edges for all the vertices in S, and similarly, let $R_Z(\overline{S})$ be the number of incoming red edges for the vertices in $\overline{S}$. From the bijection, we know the move $e = (X, Y)$ does not affect the blue tree and corresponds to, in the red tree, increasing the incoming degree of v_i by one and decreasing the incoming degree of v_{i+1} by one. Since $v_i \in \overline{S}$ and $v_{i+1} \in S$, this implies that $R_Y(S) = R_X(S) - 1$ and $R_Y(\overline{S}) = R_X(\overline{S}) + 1$.

We will now show that in Y, $R_Y(S) \geq R_X(S)$, a contradiction to $R_Y(S) = R_X(S) - 1$. First, recall that since X and Y differ by a transition on the top path they share the same blue tree and thus the same DFS ordering L. For any configuration which shares the same blue tree as X (which includes Y) we note the following. Due to the clockwise DFS order of L, all of the vertices in S have higher L values than the vertices in $\overline{S}$. Since red edges go from low to high L values, edges leaving from vertices in S must end in S. We claim that red edges leaving from vertices in P must also end in vertices in S. For the configuration X, since the path P bisects the graph, all of the red edges included in the count $R_X(S)$ originate from vertices in S or along P. Combining these implies that any configuration Z with the same blue tree as X, satisfies $R_Z(S) \geq R_X(S)$. Therefore, $R_Y(S) \geq R_X(S)$, as desired.

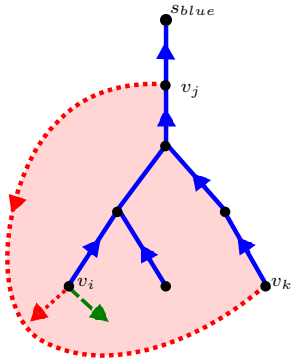

FIG. 4.11. *There is no way for the red tree path from v_i to s_{red} to leave the shaded loop since red edges go from low to high L values (L is the clockwise DFS ordering in the blue tree).*

Finally, we prove the above claim by showing that for any configuration with the same blue tree as X any red edge originating from a vertex on P ends in a vertex in S. Notice that, due to the DFS ordering, v_i (the last vertex on P) has the highest L value in $\overline{S}$ so its red edge must end in S. Consider any other vertex v_j on P and assume by contradiction that it ends in a vertex v_k in $\overline{S}$. Let P_k be the path in the blue tree between v_j and v_k. We will consider two cases. First, assume $v_k \in (\overline{S} \setminus P) \cup v_i$. Consider the closed cycle $P_k \cup \overrightarrow{v_j v_k}$. Notice that $v_i's$ red edge is contained within this cycle, but every vertex on this cycle has L value less than or equal to v_i (see Figure 4.11). This is a contradiction because there must be a red path starting with v_i's red edge and ending at s_{red} along which the L values are strictly

increasing because they increase along every red edge (there is no way for this path to leave the cycle). Next, consider the case where v_k is on $P \setminus v_i$. This argument is very similar. Consider the cycle $P_k \cup \overrightarrow{v_j v_k}$. Notice that v_k's red edge must end in a vertex on the cycle or its interior. Again because of the DFS ordering L, the vertex v_k has the highest L value on the cycle so there is no way to have a valid red path from v_k to s_{red}. This proves the claim. ∎

5. Concluding remarks. Several questions remain open. The complexity of enumerating Eulerian orientations in planar graphs of bounded degree is one of the foremost, as raised by [17]. Extending our fast mixing result to triangulations with larger degrees is a natural open problem; perhaps there is an alternate local chain which can sample efficiently from the set of 3-orientations corresponding to any fixed triangulation, without recourse to the bipartite perfect matching sampler of [20]. Finally, as mentioned previously, based on the construction we give here, Felsner and Heldt [16] recently constructed another, somewhat simpler, family of graphs for which the mixing time of $\mathcal{M}_\triangle$ and $\mathcal{M}_C$ is exponentially large. However, their family also has maximum degree that grows with n. It would be interesting to find another construction with bounded degree.

Acknowledgments. The authors thank Stefan Felsner and Daniel Held for identifying a problem with the proof of Theorem 6 that has since been addressed and an anonymous referee for suggesting simplifications and improvements to the proofs of Theorems 9 and 15.

REFERENCES

[1] I. Benjamini, N. Berger, C. Hoffman, and E. Mossel, *Mixing times of the biased card shuffling and the asymmetric exclusion process*, Trans. Amer. Math. Soc., 357 (2005), pp. 3013–3029.

[2] I. Bezakova, D. Stefankovic, V. Vazirani, and E. Vigoda, *Accelerating simulated annealing for the permanent and combinatorial counting problems*, SIAM J. Comput., 37 (2008), pp. 1429–1454, http://dx.doi.org/10.1137/050644033.

[3] P. Bhakta, S. Miracle, D. Randall, and A. Streib, *Mixing times of Markov chains for self-organizing lists and biased permutations*, in Proceedings of the 24th ACM-SIAM Symposium on Discrete Algorithms (SODA), SIAM, Philadelphia, 2013, pp. 1–15, http://dx.doi.org/10.1137/1.9781611973105.1.

[4] N. Bhatnagar and D. Randall, *Torpid mixing of simulated tempering on the Potts model*, in Proceedings of the 15th ACM-SIAM Symposium on Discrete Algorithms (SODA), SIAM, Philadelphia, 2004, pp. 478–487.

[5] N. Bonichon, *A bijection between realizers of maximal plane graphs and pairs of non-crossing Dyck paths*, Discrete Math., 298 (2005), pp. 104–114.

[6] N. Bonichon, B. Le Saëc, and M. Mosbah, *Wagner's theorem on realizers*, in Automata, Languages and Programming, Lecture Notes in Comput. Sci. 2380, Springer, Berlin, 2002, pp. 1043–1053.

[7] N. Bonichon and M. Mosbah, *Watermelon uniform random generation with applications*, Theoret. Comput. Sci., 307 (2003), pp. 241–256.

[8] E. Brehm, 3-*Orientations and Schnyder* 3-*Tree-Decompositions*, Master's Thesis, Freie Universität, Berlin, 2000.

[9] Y. Chiang, C. Chi, and H. Lu, *Orderly spanning trees with applications to graph encoding and graph drawing*, in Proceedings of the 12th ACM-SIAM Symposium on Discrete Algorithms (SODA), SIAM, Philadelphia, 2001, pp. 506–515.

[10] P. Creed, *Sampling Eulerian orientations of triangular lattice graphs*, J. Discrete Algorithms, 7 (2009), pp. 168–180.

[11] P. Diaconis and L. Saloff-Coste, *Comparison theorems for reversible Markov chains*, Ann. Appl. Probab., 3 (1993), pp. 696–730.

[12] M. Dyer and C. Greenhill, *A more rapidly mixing Markov chain for graph colorings*, Random Structures Algorithms, 13 (1998), pp. 285–317.

[13] S. Greenberg and D. Randall, *Slow mixing of Markov chains using fault lines and fat contours*, Algorithmica, 58 (2010), pp. 911–927.
[14] S. Felsner, *Convex drawings of planar graphs and the order dimension of* 3*-polytopes*, Order, 18 (2001), pp. 19–37.
[15] S. Felsner, *Geometric Graphs and Arrangements*, Vieweg & Sohn, Wiesbaden, 2004.
[16] S. Felsner and D. Heldt, *Tower Moves*, work in progress.
[17] S. Felsner and F. Zickfeld, *On the number of planar orientations with prescribed degrees*, Electron. J. Comb., 15 (2008), Research Paper R77.
[18] H. de Fraysseix and P. Ossona de Mendez, *On topological aspects of orientation*, Discrete Math., 229 (2001), pp. 57–72.
[19] M. Jerrum and A. Sinclair, *Approximate counting, uniform generation and rapidly mixing Markov chains*, Inform. Comput., 82 (1989), pp. 93–133.
[20] M. Jerrum, A. Sinclair, and E. Vigoda, *A polynomial-time approximation algorithm for the permanent of a matrix with non-negative entries*, J. Assoc. Comput. Machinery, 51 (2004), pp. 671–697.
[21] M. Jerrum, L. Valiant, and V. Vazirani, *Random generation of combinatorial structures from a uniform distribution*, Theoret. Comput. Sci., 43 (1986), pp. 169–188.
[22] D. Levin, Y. Peres, and E. Wilmer, *Markov Chains and Mixing Times*, American Mathematical Society, Providence, RI, 2006.
[23] M. Luby, D. Randall, and A. Sinclair, *Markov chain algorithms for planar lattice structures*, SIAM J. Comput., 31 (2001), pp. 167–192, http://dx.doi.org/10.1137/S0097539799360355.
[24] L. McShine and P. Tetali, *On the mixing time of the triangulation walk and other Catalan structures*, in Randomization Methods in Algorithm Design, DIMACS Ser. Discrete Math. Theoret. Comput. Sci. 43, American Mathematical Society, Providence, RI, 1999, pp. 147–160.
[25] M. Mihail and P. Winkler, *On the number of Eulerian orientations of a graph*, Algorithmica, 16 (1996), pp. 402–424.
[26] S. Miracle, D. Randall, A. Streib, and P. Tetali, *Mixing times of Markov chains on the* 3*-orientations of planar triangulations*, in DMTCS Proceedings of the 23rd International Meeting on Probabilistic, Combinatorial, and Asymptotic Methods for the Analysis of Algorithms (AofA '12), 2012, pp. 413–424.
[27] D. Randall and P. Tetali, *Analyzing Glauber dynamics by comparison of Markov chains*, J. Math. Phys., 41 (2000), pp. 1598–1615.
[28] W. Schnyder, *Embedding planar graphs on the grid*, in 1st ACM-SIAM Symposium on Discrete Algorithms (SODA), SIAM, Philadelphia, 1990, pp. 138–148.
[29] W. Schnyder, *Planar graphs and poset dimension*, Order, 5 (1989), pp. 323–343.
[30] A. Sinclair, *Algorithms for Random Generation & Counting: A Markov Chain Approach*, Birkhäuser, Boston, 1993.
[31] D. B. Wilson, *Mixing times of lozenge tiling and card shuffling Markov chains*, Ann. Appl. Probab., 14 (2004), pp. 274–325.